Network Synchronization

WILLIAM C. LINDSEY, FELLOW, IEEE, FARZAD GHAZVINIAN, MEMBER, IEEE,
WALTER C. HAGMANN, MEMBER, IEEE, AND KHALED DESSOUKY, MEMBER, IEEE

Invited Paper

Network synchronization deals with the problem of distributing time and frequency among spatially remote locations. Network synchronization is an integral part of any large communication system, such as the telephone network. It also plays an important role in many diverse applications like navigation and position determination, computer communication, data gathering, control and command systems, and phased-array antennas.

The purpose of this paper is to introduce the reader to the subject of network synchronization by organizing and presenting a tutorial of the theoretical work accomplished to date. Since the subject material is scattered, disconnected, and couched in different notations, the authors have long felt that it would be significant to organize the material and present the reader with an overview of the growth of the subject. A by-product of such a review should serve as an aid to set direction for future studies and research work.

The paper begins by providing the classification of networks into plesiochronous (asynchronous) and synchronous. Further breakdown of this basic classification into a tree-structure hierarchy is presented. Since the time and frequency waveforms transmitted between nodes experience propagation delay, some form of ranging system application is usually required in order to compensate for these delays. Several delay compensation techniques are described and incorporated into a more detailed classification of the synchronization systems. This is then followed by presenting functional network models from which a generic and unified mathematical model is formulated. Network performance measures are defined and the mathematical model is used to characterize the synchronization behavior of the network in terms of these measures. Emphasis is placed on characterizing and understanding network stability, steady-state behavior, effects of clock phase noise, and channel thermal noise. The nonlinear behavior of synchronization systems is also explored. Numerous applications are pointed out and a rather complete list (unfortunately nonexhaustive) of the references is provided for the purpose of directing future research work.

I. INTRODUCTION

Network synchronization deals with the distribution of time and frequency over a network of clocks which are spread over a wide geographical area. Fig. 1 provides the concept. The clocks are at different locations and are nor-

mally interconnected by some means as, e.g., cables or radio links. The goal is to align (synchronize) the time and frequency scales of all the clocks which belong to the network by using the data communication capacity of these links. In some applications, interest is in establishing, distributing, and maintaining a reference time as, e.g., "Greenwich Mean Time." The local time can easily be obtained by adding an appropriate offset time. Numerous applications of network synchronization are technical in nature. The following are some of the better known applications:

a) Establishing of a world-wide time distribution system.
b) Synchronization of clocks located at different multiplexing points in a digital communication network.
c) Synchronization of clocks in networks which require some form of time-division multiplexing, such as satellite networks.
d) Time distribution in a network for the purposes of network control and the performance of commands at specific times.
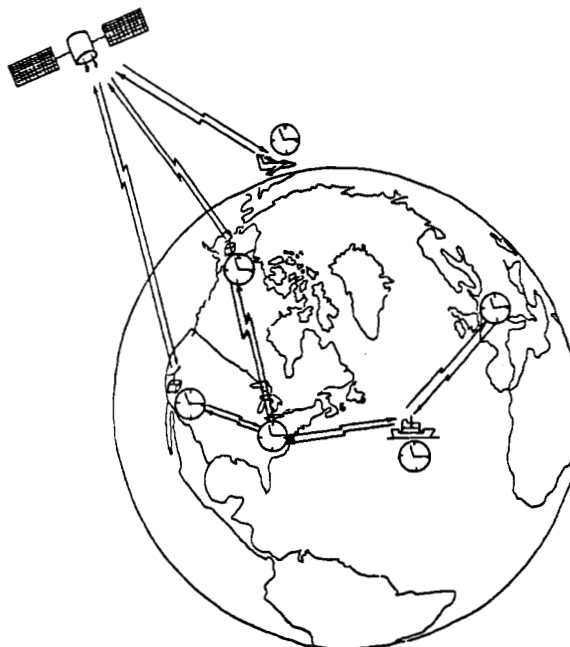

Fig. 1. An example of network of clocks.

e) Range measurement between two nodes in the network. Also position determination and navigation by the network users.
f) Establishing a supercomputer by interconnecting several computers together in a network.
g) Scientific research.
h) Phased-array antennas.

Many intriguing examples of the synchronization of a large number of oscillators can be found in nature. One of the most spectacular ones is described in a fascinating article by J. Buck and E. Buck on synchronous fireflies [1]. These fireflies flash their light organs at regular and individual intervals if they are not close together. However, if many of these insects are placed in a relatively close proximity they exhibit a synchronization of their light organs until they all flash in unison. Other biological examples are the synchronization of individual fibers in heart muscles to produce the familiar heartbeat, or the resting and active periods of mammals, which exhibit rhythms.

The mathematical treatment of network synchronization was largely stimulated by the introduction of pulse-code modulation (PCM) in the 1950s and the development of the first all-digital communication networks. Telephone companies were attracted to the use of PCM and digital communication in general for the many advantages that it offered. However, the problem with a digital communication network is that when the signals remain in digital form throughout the network, it is necessary to use time-division multiplexing and/or switching. Therefore, bits arriving at the multiplexer must be available at the right time so that the assigned time slots are filled correctly and no bits are lost. Since these bits arrive from different nodes in the network, it is essential that the clocks located at these nodes be adequately synchronized. To take advantage of the low cost of digital communication and to avoid the problem of network synchronization, telephone companies adopted the use of the pulse-stuffing technique at each multiplexing point [2]–[13]. In this technique, extra bits are added to each of the bit streams arriving at the multiplexing point to bring them to the same frequency. This allowed time-division multiplexing to be used on the bit streams. The location of these added or stuffed bits are then communicated to the other end of the link where the extra bits are removed and the bit streams are returned to their original form except for some jitter that may have been introduced by the addition and removal operations [14], [15].

Another possibility for using digital transmission while avoiding network synchronization would be to perform a digital-to-analog conversion on all the digital signals arriving at the multiplexer. These analog signals can then be multiplexed without any difficulty and the resulting signal could be digitized and transmitted to its destination. However, this method incurs additional cost due to the need for digital-to-analog and analog-to-digital converters at each multiplexer. Also, if encryption is used on the digital signals arriving at the multiplexer, the use of decryption/encryption devices is required, adding to the cost of implementation and reducing the security of the system. Another problem associated with the above methods is that they cannot be applied to networks with sources that operate at frequencies above several megahertz.

A more economical alternative to the above methods, which allows sources with higher frequencies and which also permits the signals to remain in digital form throughout the network, is to synchronize all the sources (nodes) in the network. This is what is referred to as network synchronization. By spatially synchronizing all the nodes in the network, not only the problem of time-division multiplexing is solved but also the network could be used for other applications, e.g., navigation, position determination, satellite communication, and scientific research.

Today the field of network synchronization has become very diverse and is an essential part of many facets of modern electronic communication and data gathering systems. Time transfer accuracies relate directly to the requirements of these modern systems.

II. Network Synchronization Techniques

The problem of network synchronization has been widely investigated and various methods have been proposed for achieving synchronism among a set of spatially remote clocks. It is, however, possible to categorize these methods according to the employed synchronization algorithm [16]–[21], [79], [88], [96].

Depending on the nature of the controlling signals used in obtaining synchronization, the general class of time- and frequency-transfer networks can be partitioned into two main categories; namely, plesiochronous (asynchronous) and synchronous networks, see Fig. 2. In synchronous networks all the clocks are locked in phase and frequency, whereas in plesiochronous networks no such attempt is made, however, the network consists normally of very accurate clocks which exhibit extremely small frequency offsets and drifts. The basic operating principles of these networks and some of their internal advantages and disadvantages are discussed separately below.

A. Plesiochronous Networks

In a plesiochronous network each node contains its own precise clock and there are no control signals coordinating the operation of these clocks [22], [98], see Fig. 3. Initially, the clocks are set such that the time difference between them is zero (or at least one tries to get as close to zero as possible). This calibration can be done centrally before shipping the clocks to their final locations or can be done by a "traveling clock." Since the clocks in a plesiochronous network are independent, their free-running frequencies are slightly different from each other. This frequency difference leads to a linearly increasing time error between the clocks in the network. Other factors, such as frequency drift and phase noise, also contribute to the accumulation of time errors between the nodes in the network. This time error might eventually exceed an acceptable value at which point the operation of the network should be halted and the clocks reset. The length of the time interval between updating is a function of the clock quality and the tolerable time difference between the network clocks.

The advantages of plesiochronous networks is their ease of implementation and their robustness to failures in the nodal clocks since the failure of a certain clock does not impair the performance of any other clock in the network due to their independence. The major drawback of plesio-
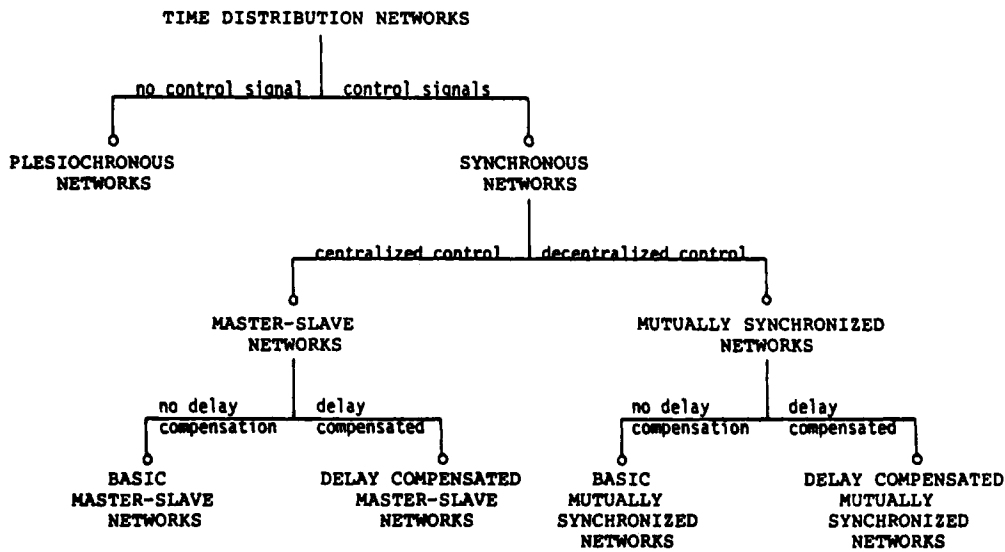
TIME DISTRIBUTION NETWORKS

no control signal | control signals

PLESIOCHRONOUS
NETWORKS

SYNCHRONOUS
NETWORKS

centralized control | decentralized control

MASTER-SLAVE
NETWORKS

MUTUALLY SYNCHRONIZED
NETWORKS

no delay
compensation

delay
compensated

no delay
compensation

delay
compensated

BASIC
MASTER-SLAVE
NETWORKS

DELAY COMPENSATED
MASTER-SLAVE
NETWORKS

BASIC
MUTUALLY
SYNCHRONIZED
NETWORKS

DELAY COMPENSATED
MUTUALLY
SYNCHRONIZED
NETWORKS

Fig. 2. Classification of time and frequency distribution networks.

chronous networks are the high purchase and maintenance costs of very accurate clocks as well as the possibility of frequent clock updating. Atomic clocks are also relatively heavy and exhibit a high power consumption which rules them out for most space applications. An example of a plesiochronous network employing cesium clocks is the TRI-TAC timing system which has an updating period of 24 h. The Global Positioning System (GPS) also employs this technique.

B. Synchronous Networks

The clocks in synchronous networks are all locked in time (phase) and frequency to a common network time and frequency, i.e., the time scales generated by spatially remote clocks are, on the average, identical. This synchronism can be achieved in several ways. The synchronization techniques employed in synchronous networks can be divided into centralized and decentralized ones depending on the nature of the control signals, see Fig. 2.

Centralized networks use the master–slave synchronization technique in which all the network clocks are either directly or indirectly slaved to a network master clock.
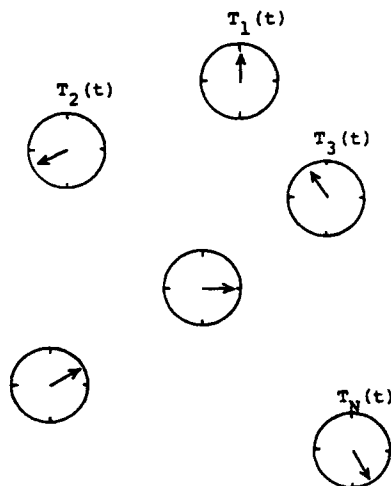

Fig. 3. A plesiochronous network.

The master clock dictates the network time scale and the network frequency. Fig. 4 shows a typical hierarchial master–slave network structure.

Decentralized networks are based on the principle of mutual synchronization. Mutually synchronized networks do not contain a master clock, instead all the clocks contribute equally to the determination of the network frequency and time scale, see Fig. 5.

1) Implementation of Master–Slave Synchronization Techniques: Of the two synchronous techniques, the master–slave synchronization technique is the better known and more widely applied [23]–[33], [74], [93]–[95]. Fig. 6 shows the operating principle of a basic two-nodal master–slave network. Clock 1 is the designated master clock and clock 2 is the slaved clock. The time scales produced by the two clocks are $T_1(t)$ and $T_2(t)$, respectively. In order to synchronize the slave clock to the master clock the latter transmits its time scale to the slave. The slave clock generates an error signal by comparing the incoming time signal $T_1(t - \tau)$ (the time scale of the master clock delayed by the transmission delay), with its own time scale $T_2(t)$ in a time difference (TD) detector. This error signal is then used to correct the slave clock.

In the steady state, the slave time scale is locked to the delayed version of the master time scale. Hence, there is a nonzero steady-state time difference between the two clocks, which depends on the transmission delay between the master and the slave clock. Any change in the transmission delay will be translated into a corresponding change in the time difference between the two clocks. If clock 2 is now used as a master to a third clock in a hierarchial structure (see Fig. 4) then the steady-state time error between clocks 1 and 3 is the sum of the time errors between clocks 1 and 2 and clocks 2 and 3.

To remove the steady-state bias between the clocks and to make their time scales less dependent on the transmission delay, one must compensate for the transmission delays between the clocks. One possible compensation technique, which is applicable if the transmission delay can be estimated, is shown in Fig. 7. The slave clock time signal is delayed by this estimate before comparing it with the received master time signal. In this way there will be no
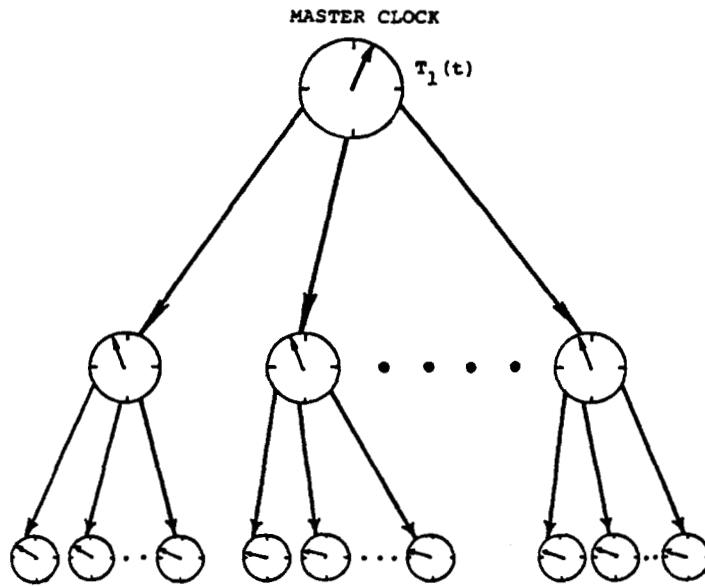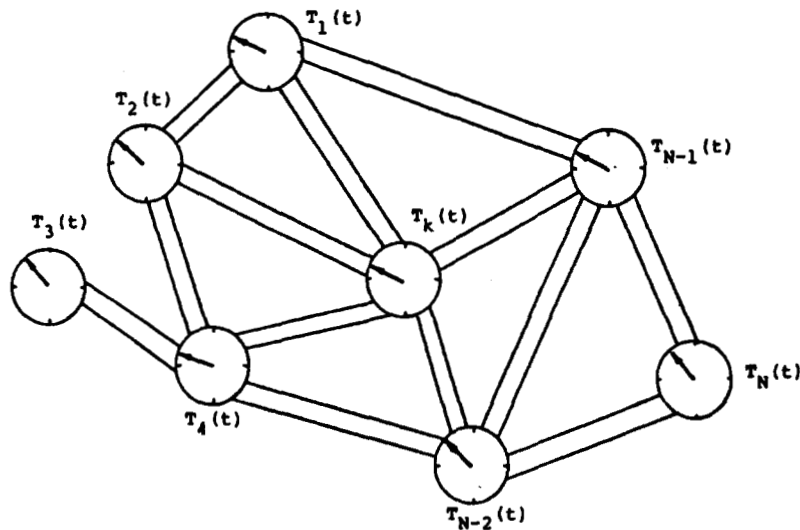
Fig. 4. A hierarchical master–slave network.

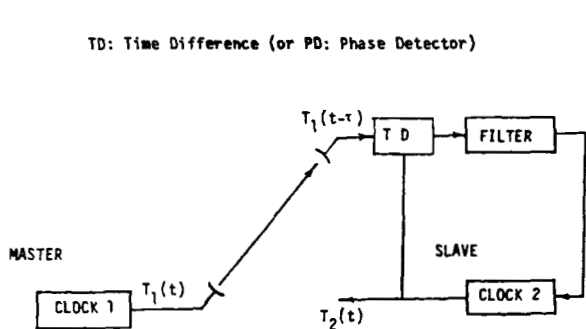Fig. 5. A partially connected mutually synchronized N-nodal network.

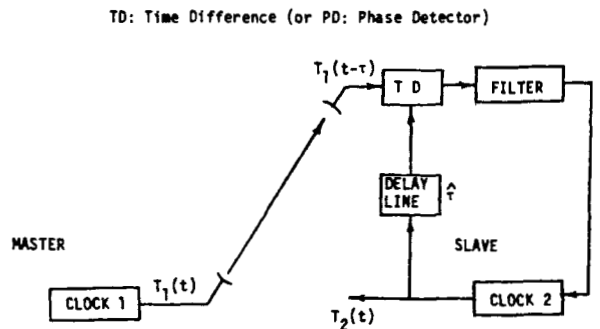Fig. 6. Block diagram of basic two-nodal master–slave network.

Fig. 7. Delay-line-compensated master–slave two-nodal network.

steady-state bias if the estimate of the delay is completely accurate. However, if the estimate is not completely accurate, as it is usually the case, the time error between the clocks depends only on the difference between the actual delay and the estimate. The delay-compensation technique just described will be referred to as delay-line compensation technique. There are other delay-compensations techniques. These are discussed in Section II-B4. An alternate approach is to phase advance the transmitted signal at each node.

One problem associated with master–slave networks is the possible loss of the master timing system. This problem can be partially corrected by designating alternate master clocks or running the slave clock independently until the master signal can be restored. The latter approach necessitates in most cases a very accurate, and therefore expensive, back-up clock at each node. Because of the potential loss of the master clock, master–slave synchronization technique is not always acceptable for military applications. On the other hand, many of the civilian communications networks, e.g., most telephone networks, prefer the master–slave method for its ease of implementation.

2) Implementation of Mutual Synchronization: As was mentioned earlier there is no master clock in a mutually synchronized network, rather it is the ensemble of clocks in the network which establishes a communication time scale. Here, each clock in the network adjusts its time (phase) so as to reduce the time error between itself and a weighted average of the rest of the network [34]–[73], [75]–[88], [90], [91], [96], [97].

Fig. 8 shows the basic operation of two mutually synchronized clocks. At each node, an error signal is generated by
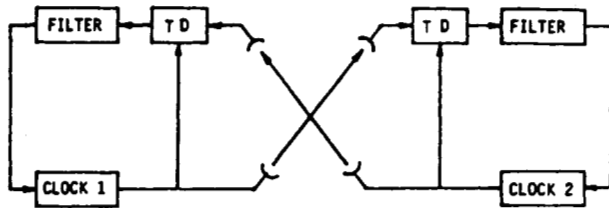
T D: Time Difference (or PD: Phase Detector)

Fig. 8. Basic mutual synchronization in a two-nodal network.

comparing the incoming time signal to the local one, as was done at the slave node in the master–slave network. This error signal is then used to correct the local clock.

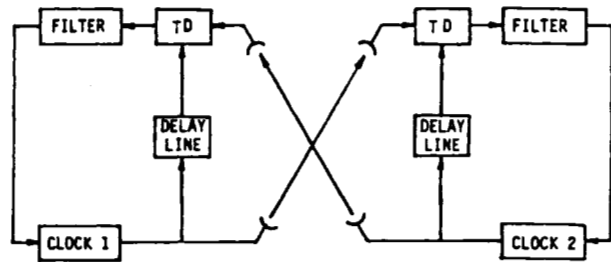T D: Time Difference (or PD: Phase Detector)

Fig. 9. Delay-line-compensated mutually synchronized two-nodal network.

As in the case of master–slave networks, the steady-state time error between the two clocks depends on the transmission delays. In addition, the steady-state network frequency depends on the transmission delays (see Section VI). Any of the delay-compensation techniques including the case discussed under the master–slave technique can be used to reduce this dependence. Fig. 9 shows the block diagram of a two-nodal delay-line compensated mutually synchronized network.

So far only two-nodal network examples have been shown. How can the clock-correction signal be obtained in a general network with an arbitrary number of nodes where some of the nodes are connected to more than one neighbor? The solution is phase averaging as shown in Fig. 10 which depicts the general nodal processing. Instead of having only one input as in Fig. 8, there are N inputs to the node shown in Fig. 10. Therefore, N time differences between the received and the local timing signals are computed. The clock-correction signal is then obtained as a weighted combination of all N error signals. Normally, it is a straightforward summation.

Fig. 11 shows the implementation which corresponds to that of Fig. 10 when delay-line compensation is used. Here the time signal of the local clock (node i) is delayed by the
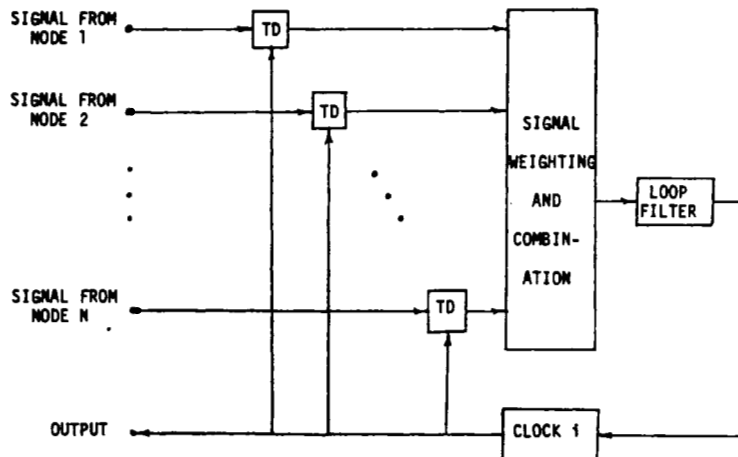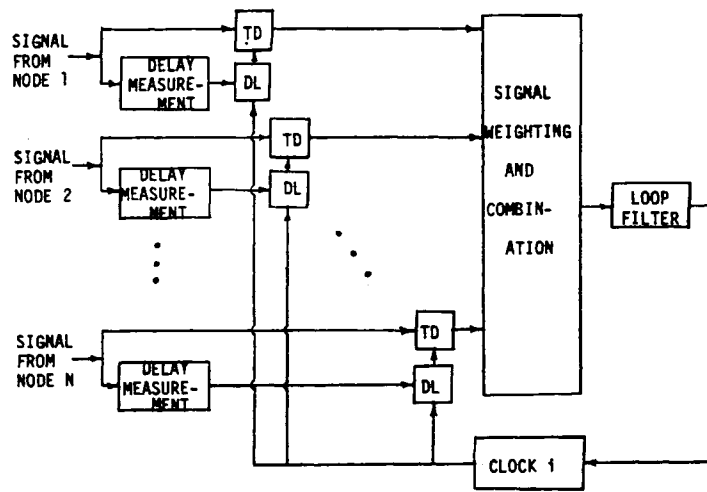
NODAL SIGNAL PROCESSING

Fig. 10. Phase averaging at node i of an N-nodal network with no delay compensation.

TD: Time Difference (or PD: Phase Detector)

DL: Delay Line

Fig. 11. Nodal processing at node *i* of an *N*-nodal network with delay compensation.

estimate of the transmission delay between node *j* and node *i* (where node *j* is connected to node *i*) and then compared with the incoming time signal from node *j*.

The advantages of mutually synchronized networks are the lack of a master clock and the fact that they are less affected by clock phase noise as compared to the other synchronization methods, as will be discussed in Section VIII. One of the problems of mutually synchronized networks is their stability associated with transients. The existence of closed loops in the networks can render them unstable for certain parameter values. However, it will be shown in Section V that these are simple conditions which can be met to ensure a stable operation.

A summary of the advantages and disadvantages of plesiochronous, master–slave, and mutual synchronization is provided in Table 1.

3) Classification of Delay Compensation Techniques: It has been pointed out already that the basic implementations of master–slave and mutual synchronization systems suffer from a transmission-delay dependence. To overcome this degradation some form of ranging system must be added to the synchronization system in order to accommodate this delay. There are several delay-compensation techniques to remedy this. Fig. 12 shows a classification of delay-compensation techniques in synchronous networks. They can be split into two subgroups depending on whether an explicit or implicit delay measurement is employed.

Explicit delay measurement implies that the transmission delay is somehow measured, possibly by means external to the synchronization system, and this value is then used in the synchronization system. Examples of a delay-compensated systems which rely on explicit delay measurement are the delay-line-compensated systems (Figs. 7 and 9) and advanced clock systems (Fig. 13). In the advanced clock method, instead of delaying the signal of the local clock and comparing it to the incoming signal, the time signal of each clock is first advanced by the measured channel delay and then transmitted to the other node.

Implicit delay measurement implies that the transmission delay is not measured internal or external to the synchronization system; however, this delay could be computed from data available within the synchronization system. All the systems in this category exchange synchronization information between the network clocks. Examples of such systems are the Equational Timing System (ETS) [59], and the Returnable Timing System (RTS) [75]. Block diagrams of these systems are shown in Figs. 14 and 15, respectively. For simplicity, the figures show two-nodal networks. The operation of these systems is described together with their mathematical models in Section III-C2.

As will be seen, delay compensation minimizes the effects of transmission delays and their variation on the performance of the synchronization network. In almost all networks of practical interest, some form of delay com-
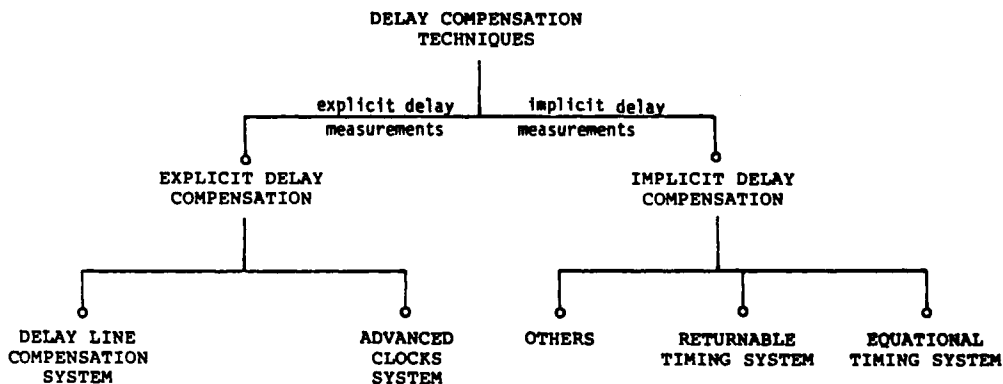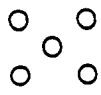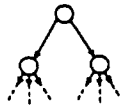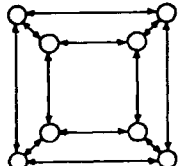

Fig. 12. Different methods of delay compensation in synchronous networks.

Table 1 Summary of the Advantages and Disadvantages of the Different Synchronization Network Structures

NETWORK STRUCTURE	ADVANTAGES	DISADVANTAGES
PLESIOCHRONOUS	• EASE OF IMPLEMENTATION • ROBUST AGAINST NODE FAILURE	• HIGHLY ACCURATE CLOCKS • FREQUENT UPDATING
MASTER-SLAVE (HIERARCHIAL)	• NO CLOSED LOOPS • SIMPLICITY OF IMPLEMENTATION	• NETWORK FREQUENCY CENTRALLY CONTROLLED BY MASTER • HIERARCHIAL CONTROL ALGORITHMS RELATED TO MASTER FAILURE • TIMING ERROR INCREASES WITH HIERARCHICAL LEVEL
MUTUAL SYNCHRONIZATION	• PROVIDES DECENTRALIZED TIME AND/OR FREQUENCY CONTROL • LOWER NODAL STABILITY REQUIREMENTS • PROVIDES SURVIVABILITY TO LEVEL OF CONNECTIVITY IMPLEMENTED • EACH NETWORK NODE HAS EQUIVALENT INFLUENCE • PHASE AND FREQUENCY INSTABILITY OF NETWORK IMPROVES WITH CONNECTIVITY IMPLYING CHEAPER NODAL CLOCKS/OSCILLATORS	• NETWORK FREQUENCY DEPENDS ON PATH DELAY DYNAMICS • REQUIRES CLOSED LOOPS • NETWORK STABILITY IS DEPENDENT ON PATH DELAY DYNAMICS • RELATIVE NODAL TIME ERRORS IS PATH DYNAMICS DEPENDENT • COMPLEXITY OF IMPLEMENTATION
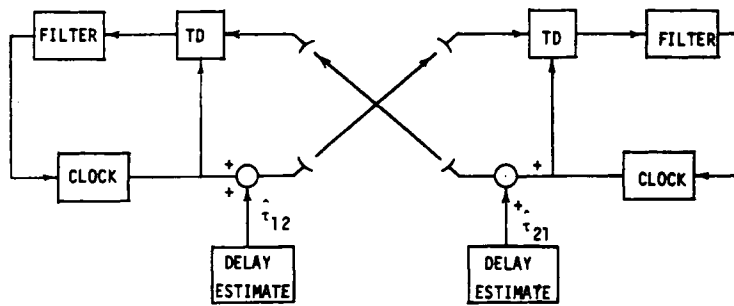
Fig. 13. A two-nodal mutually synchronized network employing advanced clock method.

pensation is necessary to achieve acceptable network synchronization performance.

4) Derivation of Synchronization Information: There are basically five different methods which can be employed to obtain the necessary synchronization information. They are:

1) burst position measurement,
2) clock time scale sampling,
3) continuous correlation of timing signals,
4) buffer fill measurement,
5) frequency difference measurement.

In the burst position measurement, the synchronized clocks are timing the transmission bursts at predetermined, repetitive, instances of time. At the reception of a data burst their actual position is compared to the nominal one. This time difference is proportional to the time difference

between the transmitting and the receiving clock plus the transmission delay. Let $T_1(t)$ and $T_2(t)$ be the time scales generated by clocks 1 and 2, respectively, the computed quantity Δ_1, at clock 1, is

$$\Delta_1 = T_2(t - \tau) - T_1(t) \tag{1}$$

where τ is the transmission delay encountered by the burst. The equivalent value at clock 2 is

$$\Delta_2 = T_1(t - \tau) - T_2(t). \tag{2}$$

In the second method, the clock time is read (sampled) at regular intervals. This value is then transmitted over a digital data link to the neighboring clock where the difference between the received clock time sample and a local clock time sample is computed. This value is again proportional to the time difference between the two clocks plus transmission and sampling delays, i.e., the computed value at

Fig. 14. Equational timing system in a mutually synchronized two-nodal network.

Fig. 15. Retunable timing system in a mutually synchronized two-nodal network.
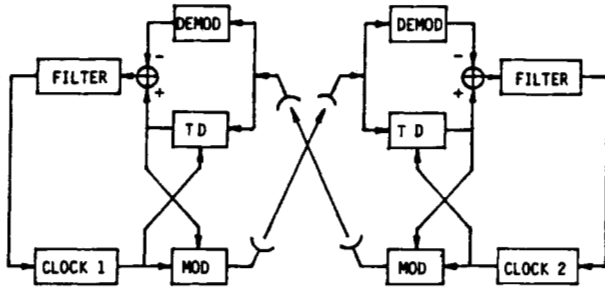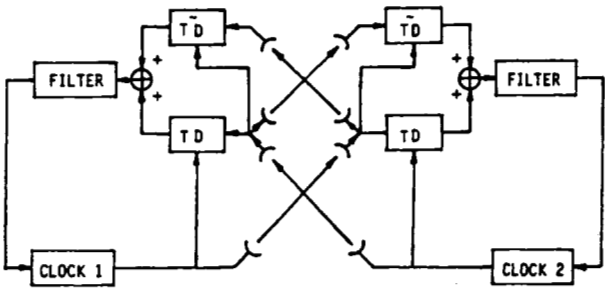
clock 1 is

$$\Delta_1 = T_2(t - \sigma) - T_1(t) \qquad (3)$$

where σ is now the sum of the transmission and data processing delays. A similar expression holds for clock 2.

The third method relies on a continuous tracking of a received timing signal at each node. One possible way to achieve this is to have each clock drive a pseudonoise (PN) sequence generator. This sequence is then transmitted. At the receiving side of the link, the PN sequence is tracked and compared to the local version in a delay locked loop. The phase offset between the received and the local PN sequence is again proportional to the time difference between the clocks plus the transmission delay as in (1).

The fourth approach is applicable in store- and forward-type data networks or in general networks in which the received data are read into a buffer by a clock derived from the data link whereas the buffer is emptied at the local clock rate. If the two clock rates are not identical then the buffer tends to fill up or to empty depending on whether the local clock rate is lower or higher than the received one. Therefore, the buffer fill status is related to the synchronism of the two clocks, and mathematically at clock 1

$$\Delta_1(t) = \int_{-\infty}^{t} [f_2(s - \tau) - f_1(s)] \, ds \qquad (4)$$

where Δ_1 is the buffer fill value at node 1 and $f_i(s)$ is the data clock rate of clock i, $i = 1, 2$. Defining

$$T_i(t) = \frac{1}{f_n} \int_{-\infty}^{t} f_i(s) \, ds \qquad (5)$$

where f_n is the nominal clock frequency, the buffer fill status can be expressed as

$$\Delta_1(t) = T_2(t - \tau) - T_1(t) \qquad (6)$$

which is equivalent to (1).

The last method employs a measurement of the frequency difference between the two clocks, i.e., at node 1 one computes

$$\Delta_1 = f_2(t - \tau) - f_1(t) \qquad (7)$$

and uses this to effect synchronous operation.

III. MATHEMATICAL MODEL OF SYNCHRONIZATION NETWORKS

Insight into the behavior of synchronization networks can only be gained through the analysis of their mathematical models. In this section, the mathematical model of a clock, which is the main building block of a synchronous network, is first presented and then this model is used to develop the mathematical model of the network.

A. Mathematical Model of a Clock

The mathematical model of a clock is the representation of the time process observed at the output of the clock. A clock is a device which consists of an oscillator and a counter. The oscillator is used to generate a cyclic waveform at a uniform rate while the counter records the number of cycles that have elapsed. The oscillator output can be modeled by a periodic waveform

$$s(t) = A(t) \sin \Phi(t) \qquad (8)$$

where

$$A(t) = A + \delta A(t). \qquad (9)$$

$\delta A(t)$ characterizes the amplitude variation about some fixed value, and t denotes the ideal time according to a reference clock. $\delta A(t)$ is usually very small and can be ignored for most timing applications. The instantaneous radian frequency function $\dot{\Phi}(t)$ can be modeled in the form

$$\dot{\Phi}(t) = \omega_0 + \sum_{k=0}^{M-1} \frac{L(k)}{k!} t^k + \dot{\xi}(t) \qquad (10)$$

where ω_0 is a constant denoting the nominal value of the free-running frequency of the oscillator. $L(0)$ is a zero-mean random variable representing the initial frequency error (departure). This error arises from the uncertainty which exists in the initial setting (setability) of the free-running frequencies of the oscillators. The $L(k)$'s ($k = 1, \cdots, M - 1$), specify a set of time-independent random variables modeling the kth-order frequency drifts, and $\dot{\xi}(t)$ is a stationary zero-mean random process characterizing the short-term oscillator instabilities.

The oscillator phase process can be obtained by integrating (10) from 0 to t. This results in

$$\Phi(t) = \Phi(0) + \omega_0 t + \sum_{k=1}^{M} \frac{L(k-1)}{k!} t^k + [\xi(t) - \xi(0)] \qquad (11)$$

for $M \geq 1$. The "time process" of the clock is obtained by dividing the oscillator phase by the nominal free-running frequency of the oscillator ω_0. Hence, the time process $T(t)$ can be written as

$$T(t) = T(0) + t + \sum_{k=1}^{M} \frac{q(k)}{k!} t^k + \Psi(t) \qquad (12)$$

where $q(k) = L(k-1)/\omega_0 (k = 1, \cdots, M)$ are a set of ran-

dom variables modeling the $(k - 1)$th-order time drifts and $\Psi(t) = \{\xi(t) - \xi(0)\}/\omega_0$ is, in general, a nonstationary stochastic process characterizing the short-term clock instabilities. Fig. 16 shows the plot of the time process $T(t)$ against the ideal time t.
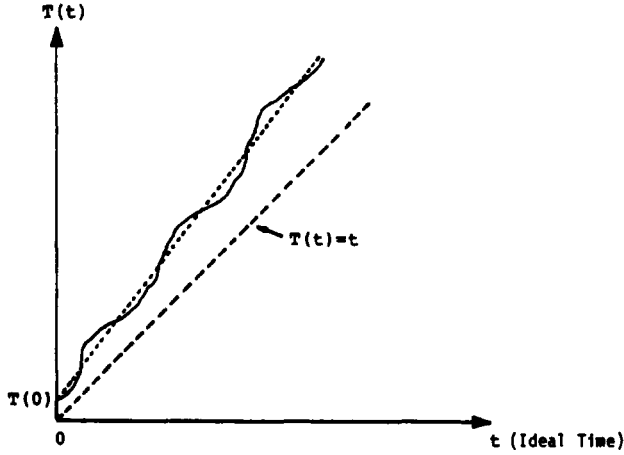

Fig. 16. Plot of the time process of a clock.

B. Mathematical Model of Plesiochronous Networks

In plesiochronous networks, the clocks are located at different geographical positions with no interconnections between them. Therefore, a clock located at node i generates a time process $T_i(t)$ which is independent of all time processes generated by other clocks in the network. $T_i(t)$ is given by (12) and is of the form

$$T_i(t) = T_i(0) + t + \sum_{k=1}^{M} \frac{q_i(k)}{k!} t^k + \Psi_i(t) \qquad (13)$$

$i = 1, 2, \cdots, N$, where N is the number of nodes in the network. The derivative of the time process $T_i(t)$ can be written as

$$\dot{T}_i(t) = 1 + \sum_{k=1}^{M} \frac{q_i(k)}{(k-1)!} t^{k-1} + \dot{\Psi}_i(t) \qquad (14)$$

$i = 1, \cdots, N$. For ease of notation, $\Omega_i(t)$ is defined as

$$\Omega_i(t) = \frac{\Phi(t)}{\omega_0} = 1 + \sum_{k=1}^{M} \frac{q_i(k)}{(k-1)!} t^{k-1} + \dot{\Psi}_i(t) \quad (15)$$

and is referred to as the normalized frequency. Therefore, the system of equations describing the operation of plesiochronous networks is given by

$$\dot{T}(t) = \Omega(t) \qquad (16)$$

where

$$\dot{T}(t) = [\dot{T}_1(t), \dot{T}_2(t), \cdots, \dot{T}_N(t)]^{tr} \qquad (17)$$

$$\Omega(t) = [\Omega_1(t), \Omega_2(t), \cdots, \Omega_N(t)]^{tr} \qquad (18)$$

and tr indicates the transpose operation on the vectors.

C. Mathematical Model of Synchronous Networks

In synchronous networks, the time process of the clock at each node is controlled by an error signal which is generated from the time signal of some or all the clocks in the network. In order to show how the general mathematical model of synchronous networks is obtained, first the math-

ematical model of a two-nodal network is developed then the results are extended to N-nodal networks.

1) Mathematical Model of Synchronous Networks with No Delay Compensation: This is the most basic model of synchronous networks. A two-nodal mutually synchronized network with no delay compensation is first considered (Fig. 8). In this network, the time signal of each clock is transmitted to the other node in the network. The received signal, which is the delayed version of the transmitted time signal, is then compared with the locally generated time signal to produce an error signal that is proportional to the time difference between the clocks in the network. This error signal is then used to control the local clock. By inspection, the equations governing the operation of this network can be written as

$$\dot{T}_1(t) = \Omega_1(t) + B_1 F_1(p)$$
$$\cdot [g_{12}[T_2(t - \tau_{12}) - T_1(t)] + N_{12}(t)] \quad (19a)$$
$$\dot{T}_2(t) = \Omega_2(t) + B_2 F_2(p)$$
$$\cdot [g_{21}[T_1(t - \tau_{21}) - T_2(t)] + N_{21}(t)] \quad (19b)$$

where B_i is the loop gain at node i, $F_i(p)$ is the loop filter at node i, $g_{ij}(\cdot)$ is the characteristics of the time (phase) detector at node j receiving time signal of node i, τ_{ij} is the delay encountered by the signal traveling from node i to node j, $N_{ij}(t)$ is the equivalent thermal noise in that channel, and $\Omega_i(t)$ is given by (15).

The mathematical model of a master–slave network, with node i as master, can be obtained from (19) by letting B_i equal zero. The mathematical model of plesiochronous networks can also be obtained from (19) by equating both B_1 and B_2 to zero.

The mathematical model of the two-nodal network presented so far can be easily generalized to N-nodal networks. (Although the generalization to N-nodal networks is not unique, the method presented here is the only one that is used in the literature.) Fig. 11 depicts the nodal processing at node i of an N-nodal network with no delay compensation. In this network, the time signal of the local clock (clock i) is compared with all the incoming time signals. The resulting error signals are then inputted to the nodal processor where a weighted average of these signals is formed to generate an error signal that is used to control the local clock. The operation of this network can be described by the following system of equations:

$$\dot{T}_i(t) = \Omega_i(t) + B_i F_i(p)$$
$$\cdot \sum_{j=1}^{N} a_{ij} \{ g_{ij}[T_j(t - \tau_{ij}) - T_i(t)] + N_{ij}(t) \} \quad (20)$$

for $i = 1, 2, \cdots, N$, where a_{ij} are normalized weighting coefficients with

$$\sum_{j=1}^{N} a_{ij} = 1 \quad \text{and} \quad a_{ii} = 0,$$

$$\text{for all } i = 1, 2, \cdots, N. \quad (21)$$

2) Mathematical Model of Synchronous Networks with Delay Compensation:

a) Delay line compensation: A two-nodal mutually synchronized network with delay line compensation is shown in Fig. 9. In this network each node estimates or measures the transmission delay between the other node and itself

and then delays the time signal of the local clock before comparing it to the arriving time signal. The mathematical model of this network is analogous to (19) and is given by

$$\dot{T}_1(t) = \Omega_1(t) + B_1 F_1(p)$$
$$\cdot \left\{ g_{12}\left[T_2(t - \tau_{12}) - T_1(t - \hat{\tau}_{12}) \right] + N_{12}(t) \right\}$$
(22a)

$$\dot{T}_2(t) = \Omega_2(t) + B_2 F_2(p)$$
$$\cdot \left\{ g_{21}\left[T_1(t - \tau_{21}) - T_2(t - \hat{\tau}_{21}) \right] + N_{21}(t) \right\}$$
(22b)

where $\hat{\tau}_{ij}$ is the estimate of τ_{ij}. For the N-nodal network with delay line compensation (Fig. 11) this becomes

$$\dot{T}_i(t) = \Omega_i(t) + B_i F_i(p)$$
$$\cdot \sum_{j=1}^{N} a_{ij}\left\{ g_{ij}\left[T_j(t - \tau_{ij}) - T_i(t - \hat{\tau}_{ij}) \right] + N_{ij}(t) \right\}$$
(23)

where $i = 1, 2, \cdots, N$.

b) Advanced clock method: The mathematical model for a two-nodal network using this compensation method (Fig. 13) can be written by inspection as follows:

$$\dot{T}_1(t) = \Omega_1(t) + B_1 F_1(p)$$
$$\cdot \left\{ g_{12}\left[T_2(t - \tau_{12}) + \hat{\tau}_{12} - T_1(t) \right] + N_{12}(t) \right\}$$
(24a)

$$\dot{T}_2(t) = \Omega_2(t) + B_2 F_2(p)$$
$$\cdot \left\{ g_{21}\left[T_1(t - \tau_{21}) + \hat{\tau}_{21} - T_2(t) \right] + N_{21}(t) \right\}.$$
(24b)

The generalization of this model to N-nodal networks is very similar to (23).

c) Equational Timing System (ETS): A method of delay compensation which has been described in the literature is the Equational Timing System (ETS) [56]–[59]. A two-nodal mutually synchronized network which uses ETS is depicted in Fig. 14. In this network, the time difference between the incoming time signal and the local time signal is measured and then its value is transmitted to the other node in the network. At each node, the control signal is formed by adding this received value of the time difference to the locally measured value of the time difference between the clocks. The mathematical model for this network is given by

$$\dot{T}_1(t) = \Omega_1(t) + F_1(p)\left[B_1 g_{12}\left[T_2(t - \tau_{12}) - T_1(t) \right] \right.$$
$$+ N_{12}(t) + \tilde{B}_1 \tilde{g}_{12}\left[T_2(t - d_{12}) \right.$$
$$\left. - T_1(t - \tau_{21} - d_{12}) \right] + \tilde{N}_{12}(t) \right]$$
(25a)

$$\dot{T}_2(t) = \Omega_2(t) + F_2(p)\left[B_2 g_{21}\left[T_1(t - \tau_{21}) - T_2(t) \right] \right.$$
$$+ N_{21}(t) + \tilde{B}_2 \tilde{g}_{21}\left[T_1(t - d_{21}) \right.$$
$$\left. - T_2(t - \tau_{12} - d_{21}) \right] + \tilde{N}_{21}(t) \right]$$
(25b)

where $\tilde{g}_{ij}[T_j(t) - T_i(t - \tau_{ij})]$ is the measurement of the difference between time signal of clock i and clock j measured at node j and transmitted to node i, and d_{ij} is the time that it takes for this value to reach node i (processing time at node j plus the transmission delay). $N_{ij}(t)$ is the equivalent noise in the transmission line between node j and i, and $\tilde{N}_{ij}(t)$ is the noise which is present in the

measurement $\tilde{g}_{ij}(\cdot)$. Equation (25) can easily be extended to obtain the mathematical model of N-nodal networks

$$\dot{T}_i(t) = \Omega_i(t) + F_i(p)$$
$$\cdot \left(B_i \sum_{j=1}^{N} a_{ij}\left[g_{ij}\left[T_j(t - \tau_{ij}) - T_i(t) \right] + N_{ij}(t) \right] \right.$$
$$+ \tilde{B}_i \sum_{j=1}^{N} b_{ij}\left[\tilde{g}_{ij}\left[T_j(t - d_{ij}) \right.\right.$$
$$\left.\left. - T_i(t - \tau_{ji} - d_{ij}) \right] + \tilde{N}_{ij}(t) \right] \right).$$
(26)

d) Returnable Timing System (RTS): Another method of compensating for transmission delays is the use of Returnable Timing System (RTS) shown in Fig. 15 [74], [75]. In this network, the output of the time detector $\widetilde{TD}$ at node 2 is proportional to the difference between the time signal from node 1 and the time signal of the local clock. The output of the time detector $\widetilde{TD}$ is proportional to the difference between the signal from clock 1 and the time signal of clock 2 returned by node 1. Therefore, the system of equations describing the operation of this network is given by

$$\dot{T}_1(t) = \Omega_1(t) + F_1(p)\left[B_1 g_{12}\left[T_2(t - \tau_{12}) - T_1(t) \right] \right.$$
$$+ N_{12}(t) + \tilde{B}_1 \tilde{g}_{12}\left[T_2(t - \tau_{12}) \right.$$
$$\left. - T_1(t - \tau_{21} - \hat{\tau}_{12}) \right] + \tilde{N}_{12}(t) \right]$$
(27a)

$$\dot{T}_2(t) = \Omega_2(t) + F_2(p)\left[B_2 g_{21}\left[T_1(t - \tau_{21}) - T_2(t) \right] \right.$$
$$+ N_{21}(t) + \tilde{B}_2 \tilde{g}_{21}\left[T_1(t - \tau_{21}) \right.$$
$$\left. - T_2(t - \tau_{12} - \hat{\tau}_{21}) \right] + \tilde{N}_{21}(t) \right]$$
(27b)

where $\tilde{g}_{ij}(\cdot)$ is the characteristic of the time detector $\widetilde{TD}$ at node i, $N_{ij}(t)$ is the equivalent noise in the transmission channel between node j and node i, and $\tilde{N}_{ij}(t)$ is the equivalent noise in the returned channel.

D. Generalized Mathematical Model of Synchronization Networks

A generalized mathematical model which can be used to describe the operation of the class of synchronous and plesiochronous networks is given by

$$\dot{T}(t) = \Omega(t) + F(p)\left[G + \tilde{G} + N + \tilde{N} \right] \cdot J \quad (28)$$

where

$$T(t) = \left[T_1(t), T_2(t), \cdots, T_N(t) \right]^{tr} \quad (29)$$

$$\Omega(t) = \left[\Omega_1(t), \Omega_2(t), \cdots, \Omega_N(t) \right]^{tr} \quad (30)$$

$$F(p) = \operatorname{diag}\left[F_1(p), F_2(p), \cdots, F_N(p) \right]_{N \times N} \quad (31)$$

$$G = \left[B_i a_{ij} g_{ij}\left[T_j(t - \tau_{ij}) - T_i(t - \eta_{ij}) + \mu_{ij} \right] \right]_{N \times N} \quad (32)$$

$$\tilde{G} = \left[\tilde{B}_i b_{ij} \tilde{g}_{ij}\left[T_j(t - \sigma_{ij}) - T_i(t - \delta_{ij}) \right] \right]_{N \times N} \quad (33)$$

$$N = \left[B_i N_{ij}(t) \right]_{N \times N} \quad (34)$$

$$\tilde{N} = \left[\tilde{B}_i \tilde{N}_{ij}(t) \right]_{N \times N} \quad (35)$$

$$J = \left[1, 1, \cdots, 1 \right]^{tr}. \quad (36)$$

The weighting coefficients a_{ij} and b_{ij} must satisfy the following conditions:

$$\sum_{j=1}^{N} a_{ij} = \sum_{j=1}^{N} b_{ij} = 1, \qquad \forall i \qquad (37)$$

and

$$a_{ii} = b_{ii} = 0, \qquad \forall i = 1, \cdots, N. \qquad (38)$$

By an appropriate choice of coefficients, (28) can be used to describe the operation of all the networks discussed so far.

1) Plesiochronous Networks: If $B_i = \tilde{B}_i = 0$, then (28) reduces to

$$\dot{T}(t) = \Omega(t) \qquad (39)$$

which is the same as (16) derived for plesiochronous networks.

2) Synchronous Networks: Equation (28) can be used to describe the operation of master–slave or mutually synchronized networks or any hybrid of both of them. In master–slave networks, the timing signal of the master clock is independent of other clocks. Therefore, if the ith clock is the master clock, the coefficients B_i and $\tilde{B}_i$ must be equal to zero. Also, in master–slave networks, the time signal of each clock is controlled only by its immediate master clock. Therefore, at node k, the coefficients $b_{kj} = a_{kj} = 0 \ \forall j \neq \ell$ and $b_{k\ell} = a_{k\ell} = 1$, where clock ℓ is the master of clock k. Any hybrid of master–slave and mutual synchronization can be represented by (28) with appropriate choices of a_{ij}, b_{ij}, B_i, and $\tilde{B}_i$.

Different delay-compensation techniques can also be represented by (28) by choosing values of η_{ij}, μ_{ij}, $\sigma_{ij}(t)$, and $\delta_{ij}(t)$.

a) No delay compensation: If there is no delay compensation, then

$$\tilde{B}_i = 0, \qquad \forall i \qquad (40)$$

and

$$\eta_{ij} = \mu_{ij} = \sigma_{ij} = \delta_{ij} = 0, \qquad \forall i, j. \qquad (41)$$

b) Delay-line compensation: In this case

$$\tilde{B}_i = 0, \qquad \forall i \qquad (42)$$

$$\eta_{ij} = \hat{\tau}_{ij}, \qquad \forall i, j \qquad (43)$$

and

$$\mu_{ij} = \sigma_{ij} = \delta_{ij} = 0, \qquad \forall i, j. \qquad (44)$$

c) Advance clock method: For these networks

$$\tilde{B}_i = 0, \qquad \forall i \qquad (45)$$

$$\mu_{ij} = \hat{\tau}_{ij}, \qquad \forall i, j \qquad (46)$$

and

$$\eta_{ij} = \sigma_{ij} = \delta_{ij} = 0, \qquad \forall i, j. \qquad (47)$$

d) Equational Timing System (ETS): To represent this delay-compensation technique, it is required that

$$\mu_{ij} = \eta_{ij} = 0, \qquad \forall i, j \qquad (48)$$

$$\sigma_{ij} = d_{ij}, \qquad \forall i, j \qquad (49)$$

and

$$\delta_{ij} = \tau_{ji} + d_{ij}, \qquad \forall i, j. \qquad (50)$$

e) Returnable Timing System (RTS): For this case

$$\mu_{ij} = \eta_{ij} = 0, \qquad \forall i, j \qquad (51)$$

$$\sigma_{ij} = \tau_{ij}, \qquad \forall i, j \qquad (52)$$

$$\delta_{ij} = \hat{\tau}_{ij} + \tau_{ji}, \qquad \forall i, j. \qquad (53)$$

E. Linearized Mathematical Model of Synchronization Networks

Analysis of the mathematical model in its most general form given in (28) is a difficult analytical problem. For several of the network performance measures (to be described in the following section) it is sufficient to consider the linearization of the model of (28). In the linearized model, the functions $g_{ij}(\cdot)$ and $\tilde{g}_{ij}(\cdot)$ are assumed linear. This assumption can be well justified by the use of PN sequences, or by assuring that the phase detectors are operating in the linear region of their characteristic curves. The linearized mathematical model of the time process at node i is given by

$$\dot{T}_i(t) = \Omega_i(t) + F_i(p)$$

$$\cdot \left(B_i \sum_{j=1}^{N} a_{ij} \left[\left[T_j(t - \tau_{ij}) - T_i(t - \eta_{ij}) \right] \right. \right.$$

$$+ \mu_{ij} + N_{ij}(t) \right] + \tilde{B}_i \sum_{j=1}^{N} b_{ij} \left[\left[T_j(t - \sigma_{ij}) \right. \right.$$

$$\left. \left. - T_i(t - \delta_{ij}) \right] + \tilde{N}_{ij}(t) \right] \right). \qquad (54)$$

IV. Network Performance Measures

The performance of the various network synchronization methods can only be judged and compared on a set of meaningful measures tailored to the intended application. However, these measures have to be general enough such that they can be evaluated for different implementations.

The measures which are discussed here can be divided into two major categories. The first category includes performance measures to judge the steady-state behavior of the synchronization system under relatively ideal conditions. They result in an estimation of the basic limits of the systems as a function of several nonrandom network parameters, e.g., the free-running clock frequencies and the transmission delays. These performance measures are very crude and are merely an indication as to whether a particular synchronization system is worth the effort of any further investigation. The performance measures in this category are:

a) Steady-State Network Behavior: The steady-state network behavior is an indication of the basic limitations of the network in an ideal environment such as constant delays, no oscillator instabilities, and in fact, no channel noise. It shows how the network parameters and connectivity influence such values as the network frequency and the time errors between nodal clocks.

b) Network Stability: Network stability deals with the decay of transients in the network. Two sets of results can be obtained in analytical form. The first is a set of sufficient conditions, formulated as a function of network parameters, like delays, gains, etc., to guarantee decaying network transients. The second set of results deals with the rate at which these transients decay as a function of the network parameters and the topology (connectivity between the clocks).

The second category contains the statistical performance measures dealing with the accuracy of the time and frequency distribution in the network in the presence of random disturbances and noise processes. These performance measures are:

a) *Time Error Process:* This is defined as

$$T_{ij}(t) \triangleq T_i(t) - T_j(t), \qquad i,j = 1,\cdots,N; i \neq j. \quad (55)$$

This time difference should ideally be zero. Oscillator frequency instabilities and phase noise, channel thermal noise, and topological changes, however, make it a random process. This process will have values dispersed about a mean value which may not be zero. This performance measure is particularly important when a common time base has to be established in a network, e.g., in very long baseline interferometry or world-wide time distribution.

Another version of this performance measure using the phase counterparts of the time process in (55) is also used. The phase error between the nodes is defined as

$$\Phi_{ij}(t) \triangleq \Phi_i(t) - \Phi_j(t), \qquad i,j = 1,\cdots,N; i \neq j \quad (56)$$

where $\Phi_i(t)$ is the phase at the output of the oscillator in the ith node at some time t. ($\Phi_{ij}(t)$ has also been denoted by $\Delta\Phi_{ij}(t)$ in the literature.) This process is also referred to as the "space increment" of the nodal phase processes. Space in this context refers to the spatial difference or geographical separation of the nodes under consideration.

b) *Time Interval Process:* A time interval of length h as observed on the time scale at node i is given by

$$\Delta T_i(t; h) = T_i(t + h) - T_i(t), \qquad i = 1,\cdots,N. \quad (57)$$

This process should ideally be equal to the value h at all t. The instabilities and noises in the network diffuse it and can even make its expected value not equal to h.

The phase version of (57) is defined as

$$\Delta\Phi_i(t; h) = \Phi_i(t + h) - \Phi_i(t), \qquad i = 1,\cdots,N. \quad (58)$$

This process is referred to as the "time increment" of the phase process at node i.

c) *Time Interval Error Process:* The time interval error means the difference in the measurement of a time interval, say of length h, at one node and the measurement of the same interval at another node. It is defined as follows:

$$\Delta T_{ij}(t; h) \triangleq \left[T_i(t + h) - T_i(t) \right] - \left[T_j(t + h) - T_j(t) \right]. \quad (59a)$$

Using (57), this can be written as the difference between the time interval processes at nodes i and j

$$\Delta T_{ij}(t; h) = \Delta T_i(t; h) - \Delta T_j(t; h). \quad (59b)$$

Or using (55) it can be written as the difference of the time error processes at time $t + h$ and time t

$$\Delta T_{ij}(t; h) = T_{ij}(t + h) - T_{ij}(t). \quad (59c)$$

From the definition, the ideal mean value of the time interval error process is zero. However, as we shall see, certain oscillator instabilities can lead to nonzero mean time interval error. This indicates that one of the oscillators under consideration is either faster or slower than the other. As such, this performance measure characterizes the accuracy of the frequency transfer in the network. Time interval error is a CCITT approved performance measure for plesiochronous networks.

The phase version of this performance measure is defined in a similar manner as

$$\Delta\Phi_{ij}(t; h) \triangleq \Phi_{ij}(t + h) - \Phi_{ij}(t) \quad (60)$$

and is referred to as the "space and time increment" of the phase processes at nodes i and j.

In the sections to follow, the different performance measures described herein will be used to develop an understanding of the characteristics of synchronization networks.

V. NETWORK STABILITY

This section deals with the stability of synchronous networks and how it is influenced by the network parameters and the network topology. Stability, as used in this section, deals with the behavior of transients in the network, viz., the conditions under which transients decay and at which rate the transient decay is taking place. The goal of this section is to show in a very rudimentary form, the methods which have been employed in the literature to obtain information on the stability of synchronized clocks. The interested reader is referred to more detailed treatments in the literature [99]–[102]. It has been shown earlier that the network can be described by a linearized set of equations for most cases of interest. Therefore, the stability of the network synchronization systems can be discussed by elementary Laplace transform methods. However, analytical results are still not easily obtained due to the large number of parameters and the nonzero transmission delays between the network nodes. In the most general case, i.e., in the absence of any restricting assumptions on the network topology, it is only possible to develop sufficient stability conditions. Analytical results giving the approximate locations of dominant system poles can only be obtained for a restricted subclass of network topologies in which all the transmission delays between the connected nodes are equal.

A. Sufficient Stability Conditions

Taking the Laplace transform of the linearized mathematical model in (44) the network can be described in the Laplace domain by the matrix equation

$$Q(s) \cdot T(s) = P(s) \quad (61)$$

where $Q(s)$ is an $N \times N$ matrix, $P(s)$ and $T(s)$ are N-vectors. $T(s)$ is the vector of the Laplace transforms of the nodal time scales, i.e., it is the desired system output, and $P(s)$ is a vector with no poles in $R^+ = \{ s: \mathrm{Re}(s) \geq 0, s \neq 0 \}$. Equation (61) can be solved for $T(s)$ if $Q^{-1}(s)$ exists. The derivation of the sufficient stability conditions are based on the existence of $Q^{-1}(s)$, in particular on the following theorem:

Theorem 5.1: Let $Q(s) = [q_{ik}]_{N\times N}$ be a complex matrix which is diagonally dominant in R^+, i.e.,

$$|q_{ii}| > \sum_{\substack{j=1 \\ j \neq i}}^{N} |q_{ij}|, \qquad i = 1, 2, \cdots, N \quad (62)$$

then the roots of $\det[Q(s)]$ have negative real parts with the possible exception of roots at the origin.

The proof of this theorem is given in [39]. Sufficient condition can now be obtained from (62) after some tedious but straightforward algebra [97]. The results are shown in Table

Table 2 Sufficient Conditions for the Stability of Synchronous Networks

Network Type	No Loop Filter	$F_k(s) = \dfrac{1}{1 + \rho_k s}$
Master–Slave Networks	always stable	
Mutually Synchronized with no Delay Compensation	always stable	$B_k \cdot \rho_k < 1/2, \quad \forall k$
Mutually Synchronized with Delay Line Compensation	$B_k \cdot \hat{\tau}_{k\ell} < 1/2, \quad \forall k^*$	$B_k[\hat{\tau}_{k\ell} + \rho_k] < 1/2, \quad \forall k^*$
Mutually Synchronized with ETS or RTS[†]	$B_k \cdot \delta_{k\ell} < \sqrt{2} - 1, \quad \forall k^{**}$	$B_k[\delta_{k\ell} + \rho_k] < \sqrt{2} - 1, \quad \forall k^{**}$ (Miller)

$$^*\hat{\tau}_{k\ell} = \max_{j \neq k} \hat{\tau}_{kj}$$
$$^{**}\delta_{k\ell} = \max_{j \neq k} \delta_j$$
$$^{\dagger}\delta_{kj} = \hat{\tau}_{kj} + \tau_{jk}, \quad \text{for RTS}$$
$$\delta_{kj} = d_{kj} + \tau_{jk}, \quad \text{for ETS.}$$

2 for various types of delay compensation methods as discussed in Section II-B3, in the presence and absence of a first-order Butterworth filter in the local feedback loops.

The results indicate that there is an upper limit for the gain-delay product (channel delay times the open-loop gain in the nodal phase locked loops) to assure system stability.

B. Approximate Pole Locations for Dominant Poles

An important consideration in synchronous networks is the rate at which the transients die down. This result cannot be obtained from the sufficient conditions since they only guarantee that all the system poles are in the left half plane but do not give the position of these poles.

Analytical results for the dominant pole location can only be obtained for a special subclass of network topologies, in particular it has to be assumed that all the delays between the connected nodes are equal, all nodal loop gains are equal, and no nodal loop filters are employed. With respect to the general noise-free linear model in (54) it is required that

$$\tau_{ij} = \sigma_{ij} = \delta_{ij}/2 = \tau, \quad \forall i,j: i \leftrightarrow j$$
$$a_{ij} = b_{ij}, \quad \forall i,j$$
$$B_i = \tilde{B}_i = B, \quad \forall i$$
$$F_i(s) = 1, \quad \forall i$$

in which case the mathematical model takes the form of the matrix differential-difference equation:

$$\dot{T}(t) = \Omega(t) - BT(t) + 2BAT(t - \tau) - BT(t - 2\tau) \tag{63}$$

where $A = [a_{ij}]_{N \times N}$ is the network weighting matrix. If the matrix A can be diagonalized in the form

$$A = U\Lambda U^{-1}$$
$$\Lambda = \text{diag}(\lambda_1, \lambda_2, \cdots, \lambda_N)$$

then the set of differential-difference equations in (63) can be decoupled by the transformation

$$X(t) = U^{-1}T(t)$$

into

$$\dot{X}(t) = U^{-1}\Omega(t) - BX(t) + 2B\Lambda X(t - \tau) - BX(t - 2\tau). \tag{64}$$

Under the aforementioned conditions it is possible to decompose the N-dimensional problem into a decoupled set of N one-dimensional problems. The network stability can now be studied via the dominant poles of the characteristic equations associated with the homogeneous part of (64). The normalized characteristic quasi-polynomials associated with (64) are given by

$$\psi(s) = 1 + s - 2\lambda_i e^{-s\gamma} + e^{-2s\gamma} \tag{65}$$

where $\gamma = B \cdot \tau$ is the gain-delay product which has already played an important role in the sufficient stability conditions. It can be shown that the eigenvalues λ_i of the weighting matrix A satisfy the condition $|\lambda_i| \leq 1$, $i = 1, 2, \cdots, N$. Given the specific eigenvalues λ_i it is now possible to numerically solve the characteristic equation $\psi(s) = 0$ for the dominant pole. No analytical solution is possible at this point and one has to resort to numerical methods. Fig. 17 shows the location of the dominant poles associated with four real eigenvalues. Similar plots can be generated for complex eigenvalues [97]. The value of the gain-delay product γ is increasing in the direction of the arrows; three specific values of γ are marked in Fig. 17. Notice that the set of eigenvalues $\{\lambda_i\}$ reflects the network topology whereas γ reflects the influence of the transmission delays between the nodes. Fig. 18 shows the behavior of the real part of the dominant poles as a function of the logarithm of the gain-delay product γ. The figure shows that there exists an optimum value of the gain-delay product for which the dominant pole is located a maximum amount into the left half plane.

This optimum point is a function of the network topology, since the topology influences the set of eigenvalues of the weighting matrix A. In the case of equal delay networks it is possible to find a more accurate sufficient stability condition than the one presented in Section V-A for an arbitrary network. The derivation is too lengthy to be included here. The interested reader is referred to [97]. It is
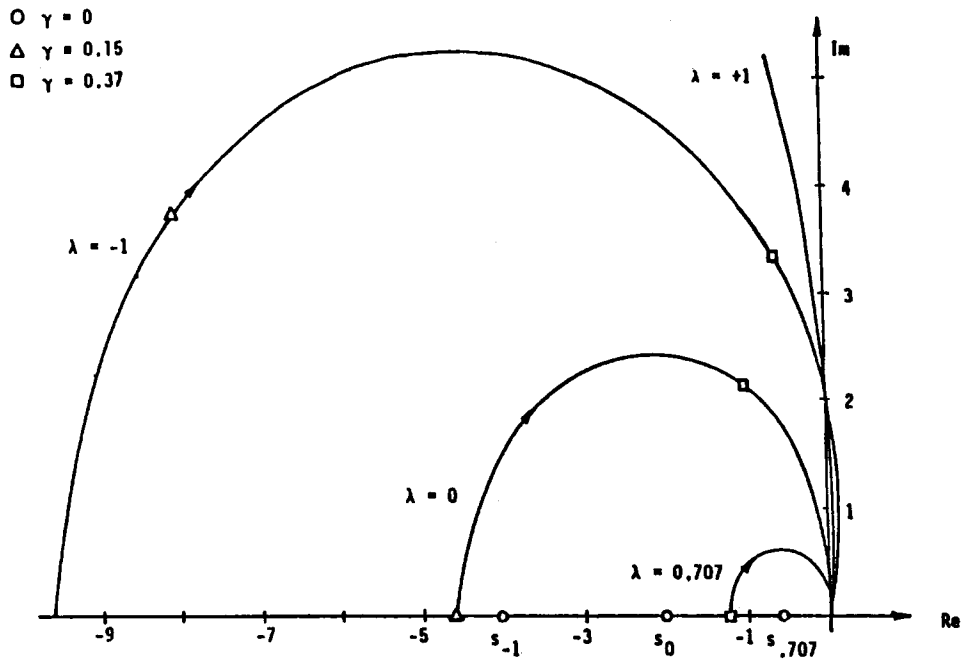
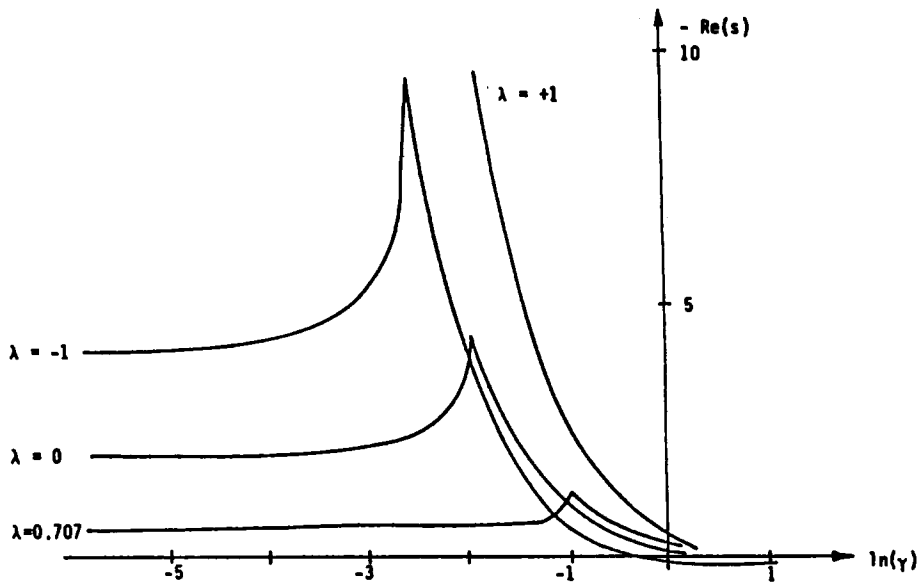**Fig. 17.** Location of dominant network poles for real eigenvalues.

Fig. 18. Real part of dominant poles versus gain-delay product.

shown there that the bound given in Section V-A is very conservative in case that the weighting matrix A has only real eigenvalues. However, the same bound becomes tight in cases where A has complex eigenvalues near the unit circle.

VI. STEADY-STATE BEHAVIOR OF SYNCHRONOUS NETWORKS

Steady-state network behavior is a basic performance measure of synchronous networks which deals with the operation of the network after the transients have decayed. In determining steady-state behavior, it is always assumed that the network is stable and that there is no clock instability or channel noise present.

In the steady state, the parameters of interest are the steady-state frequency of the clocks and the time error between them. These parameters indicate the basic limitations of a network and can be used as comparative measures between different networks.

The linearized mathematical model of the network is given by (54). The assumption that there are no short-term or long-term clock instabilities present implies that $\Omega_i(t)$ is constant. Furthermore, it is assumed that there are no channel noise or loop filters in the network (the results will hold for networks with loop filters if the filters satisfy the condition

$$\lim_{s \to 0} F_i(s) = 1, \qquad \forall i$$

where $F_i(s)$ is the transfer function of the loop filter in the ith node). Therefore, the mathematical model of the network is given by

$$\dot{T}_i(t) = \Omega_i + B_i \sum_{j=1}^{N} a_{ij} \left[T_j(t - \tau_{ij}) - T_i(t - \eta_{ij}) + \mu_{ij} \right]$$

$$+ \tilde{B}_i \sum_{j=1}^{N} b_{ij} \left[T_j(t - \sigma_{ij}) - T_i(t - \delta_{ij}) \right], \qquad \forall i. \quad (66)$$

If the network is assumed to be stable with its steady-state frequency (this is in fact the normalized frequency) denoted by Ω_s, then

$$\lim_{t \to \infty} \dot{T}_i(t) = \Omega_s, \qquad \forall i. \tag{67}$$

The time process $T_i(t - \tau_{ij})$ can in general be written as

$$T_i(t - \tau_{ij}) = T_i(t) - \int_{t-\tau_{ij}}^{t} \dot{T}_i(x)\, dx. \tag{68}$$

In the steady state, $\dot{T}_i(x) = \Omega_s$, therefore (68) reduces to

$$T_i(t - \tau_{ij}) = T_i(t) - \Omega_s \tau_{ij}. \tag{69}$$

Substituting (69) in (66) results in

$$\Omega_s \frac{1 + \beta_i}{B_i + \tilde{B}_i} = \frac{\Omega_i}{B_i + \tilde{B}_i} - T_i(t)$$

$$+ \sum_{j=1}^{N} \frac{B_i a_{ij} + \tilde{B}_i b_{ij}}{B_i + \tilde{B}_i} T_j(t) + \frac{\gamma_i}{B_i + \tilde{B}_i} \tag{70}$$

where

$$\beta_i = B_i \sum_{j=1}^{N} a_{ij}(\tau_{ij} - \eta_{ij}) + \tilde{B}_i \sum_{j=1}^{N} b_{ij}(\sigma_{ij} - \delta_{ij}) \tag{71}$$

and

$$\gamma_i = B_i \sum_{j=1}^{N} a_{ij}\mu_{ij}. \tag{72}$$

The matrix representation of (70) is given by

$$\Omega_s X = \Omega_B + CT(t) + \gamma \tag{73}$$

where

$$X = \left[\frac{1 + \beta_1}{B_1 + \tilde{B}_1}, \frac{1 + \beta_2}{B_2 + \tilde{B}_2}, \cdots, \frac{1 + \beta_N}{B_N + \tilde{B}_N} \right]^{tr} \tag{74}$$

$$\Omega_B = \left[\frac{\Omega_1}{B_1 + \tilde{B}_1}, \frac{\Omega_2}{B_2 + \tilde{B}_2}, \cdots, \frac{\Omega_N}{B_N + \tilde{B}_N} \right]^{tr} \tag{75}$$

$$T(t) = \left[T_1(t), T_2(t), \cdots, T_N(t) \right]^{tr} \tag{76}$$

$$\gamma = \left[\frac{\gamma_1}{B_1 + \tilde{B}_1}, \frac{\gamma_2}{B_2 + \tilde{B}_2}, \cdots, \frac{\gamma_N}{B_N + \tilde{B}_N} \right]^{tr} \tag{77}$$

and C is the connectivity matrix of the network with

$$c_{ij} = \begin{cases} -1, & i = j \\ \dfrac{B_i a_{ij} + \tilde{B}_i b_{ij}}{B_i + \tilde{B}_i}, & i \neq j \end{cases} \quad 1 \leqslant i, j \leqslant N. \tag{78}$$

It can be easily shown that the connectivity matrix of a connected network has rank $(N - 1)$. Therefore, there exists a vector Y such that

$$Y^{tr} C = 0^{tr} \tag{79}$$

where 0 is a vector of all zeros. The steady-state frequency of a network is obtained by multiplying both sides of (73) by Y^{tr} and is given by

$$\Omega_s = \frac{Y^{tr}\Omega_B + Y^{tr}\gamma}{Y^{tr}X}. \tag{80}$$

Equation (80) gives a general formula for calculating the steady-state frequency of any network with arbitrary connectivity.

The steady-state time error between the nodes in the network can also be found from (73). This is done by choosing one of the clocks in the network as a reference clock and then calculating the time error between this clock and the rest of the clocks in the network. If the steady-state time error between the reference clock and clock i is denoted by $T_{ri}, 1 \leqslant r \leqslant N$, then (73) can be written as

$$CT_r = \Omega_B - \Omega_s X + \gamma \tag{81}$$

where

$$T_r = \left[T_{r1}, T_{r2}, \cdots, T_{rN} \right]^{tr}. \tag{82}$$

Since the rank of the matrix C is $(N - 1)$, it does not have an inverse and therefore T_r cannot be found directly from (81). However, by definition $T_{rr} = 0$, and hence the rth equation in (81) can be eliminated, leaving $(N - 1)$ equations. The steady-state time error can now be evaluated from

$$\tilde{T}_r = \tilde{C}^{-1} \left[\tilde{\Omega}_B - \Omega_s \tilde{X} + \tilde{\gamma} \right] \tag{83}$$

where $\tilde{T}_r$, $\tilde{X}$, $\tilde{\Omega}_B$, and $\tilde{\gamma}$ are obtained by deleting the rth row of T_r, X, Ω_B, and γ, respectively, and $\tilde{C}$ is obtained by deleting the rth row and the rth column of C.

To gain better insight into how network structure and the synchronization technique employed by the network affect its steady-state behavior, the steady-state frequency and time error of fully connected mutually synchronized network and a hierarchical master–slave network are evaluated and the results are shown in Tables 3–5.

In obtaining the steady-state frequency for the fully connected network given in Table 3, it is assumed that the weighting coefficients at all nodes are equal. As it can be seen from this table, the steady-state frequency for the network with no delay compensation depends on the transmission delay between the nodes. With the use of delay-compensation techniques, this dependence is either eliminated or reduced considerably. The same effect can be

Table 3 Steady-State Frequency of a Fully Connected Mutually Synchronized Network of N Nodes

Network Configuration	Steady-State Frequency Ω_s
No Delay Compensation	$\dfrac{\sum\limits_{i=1}^{N} \Omega_i/B_i}{\sum\limits_{i=1}^{N} 1/B_i + \dfrac{1}{N-1} \sum\limits_{i=1}^{N} \sum\limits_{\substack{j=1 \\ j \neq i}}^{N} \tau_{ij}}$
Delay-Line Compensation	$\dfrac{\sum\limits_{i=1}^{N} \Omega_i/B_i}{\sum\limits_{i=1}^{N} 1/B_i + \dfrac{1}{N-1} \sum\limits_{i=1}^{N} \sum\limits_{\substack{j=1 \\ j \neq i}}^{N} \Delta\tau_{ij}}$
Equational Timing System	$\dfrac{\sum\limits_{i=1}^{N} \Omega_i/B_i}{\sum\limits_{i=1}^{N} 1/B_i}$
Returnable Timing System	$\dfrac{\sum\limits_{i=1}^{N} \Omega_i/B_i}{\sum\limits_{i=1}^{N} 1/B_i + \dfrac{1}{N-1} \sum\limits_{i=1}^{N} \sum\limits_{\substack{j=1 \\ j \neq i}}^{N} \Delta\tau_{ij}}$

Table 4 Steady-State Time Error Between the Nodes of a Fully Connected Mutually Synchronized Network of N Nodes

Network Configuration	Steady-State Time Error T_{ri}
No Delay Compensation	$\dfrac{N-1}{N}\left[\dfrac{\Omega_r - \Omega_i}{B}\right] - \dfrac{1}{N}\Omega_s\left[\displaystyle\sum_{\substack{j=1\\j\neq r}}^{N}\tau_{rj} - \sum_{\substack{j=1\\j\neq i}}^{N}\tau_{ij}\right]$
Delay-Line Compensation	$\dfrac{N-1}{N}\left[\dfrac{\Omega_r - \Omega_i}{B}\right] - \dfrac{1}{N}\Omega_s\left[\displaystyle\sum_{\substack{j=1\\j\neq r}}^{N}\Delta\tau_{rj} - \sum_{\substack{j=1\\j\neq i}}^{N}\Delta\tau_{ij}\right]$
Equational Timing System	$\dfrac{N-1}{N}\left[\dfrac{\Omega_r - \Omega_i}{B}\right] - \dfrac{1}{N}\Omega_s\left[\displaystyle\sum_{\substack{j=1\\j\neq r}}^{N}(\tau_{rj} - \tau_{jr}) - \sum_{\substack{j=1\\j\neq i}}^{N}(\tau_{ij} - \tau_{ji})\right]$
Returnable Timing System	$\dfrac{N-1}{N}\left[\dfrac{\Omega_r - \Omega_i}{B}\right] - \dfrac{1}{N}\Omega_s\left[\displaystyle\sum_{\substack{j=1\\j\neq r}}^{N}[\Delta\tau_{rj} + (\tau_{rj}-\tau_{jr})] - \sum_{\substack{j=1\\j\neq i}}^{N}[\Delta\tau_{ij} + (\tau_{ij}-\tau_{ji})]\right]$

Table 5 Steady-State Time Error Between Master Clock and Clock i in the Hierarchical Master–Slave Network of N Nodes. Ω_{mas}: Frequency of Master Clock, $\Omega_s = \Omega_{mas}$

Network Configuration	Steady-State Time Error T_{1i}
No Delay Compensation	$\displaystyle\sum_{j\in M_i}(\Omega_{mas} - \Omega_j)/B_j + \Omega_{mas}\sum_{\substack{j\in M_i\\k\to j}}\tau_{jk}$
Delay-Line Compensation	$\displaystyle\sum_{j\in M_i}(\Omega_{mas} - \Omega_j)/B_j + \Omega_{mas}\sum_{\substack{j\in M_i\\k\to j}}\Delta\tau_{jk}$
Equational Timing System	$\displaystyle\sum_{j\in M_i}(\Omega_{mas} - \Omega_j)/2B_j + \frac{\Omega_{mas}}{2}\sum_{\substack{j\in M_i\\k\to j}}(\tau_{jk} - \tau_{kj})$
Returnable Timing System	$\displaystyle\sum_{j\in M_i}(\Omega_{mas} - \Omega_j)/2B_j + \frac{\Omega_{mas}}{2}\sum_{\substack{j\in M_i\\k\to j}}[\Delta\tau_{jk} + (\tau_{jk} - \tau_{kj})]$

observed in the results obtained for the steady-state time error between the nodes given in Table 4. For example, in the case of the delay-line compensation technique when the estimates of the transmission delays are exact, then the steady frequency and time error of the network are completely independent of the transmission delays and are given by

$$\Omega_s = \frac{\sum_{i=1}^{N}\Omega_i/B_i}{\sum_{i=1}^{N}1/B_i} \qquad (84)$$

and

$$T_{r_i} = \frac{N-1}{N}\left[\frac{\Omega_r - \Omega_i}{B}\right]. \qquad (85)$$

In the case of the hierarchical master–slave networks (see Fig. 4) the steady-state frequency of the network is equal to the frequency of the master clock, and the time error between the master clock and other clocks in the network is given in Table 5. In this table M_i denotes the set of all the master clocks of node i in the hierarchical structure including clock i itself and $k \to j$ indicates the value of k for which clock k is the immediate master of clock j. It is clear from the structure of this network that for each j, only one value of k can exist, except for $j = 1$ where clock 1

does not have a master. It can be seen from this table that the steady-state time error between the master clock and a clock in the network accumulates as the clock moves down in the hierarchy. Also, as the clock moves further down the hierarchy, its time process becomes more dependent on the transmission delays. This property is one of the major drawbacks of hierarchical master–slave networks. To reduce the buildup of time error in the network and to lessen the dependence on the channel delays, a delay-compensation technique must be employed. The results given for the delay-compensation technique in Table 5 indicate the reduction in the time error buildup and reduced effect of the transmission delays.

VII. Effects of Long-Term Clock Instabilities

In deriving the steady-state behavior of the network it was assumed that there are no long-term clock instabilities present in the model of the network clocks. Therefore, the steady-state time error between the nodes of the network was found to be independent of time. However, in practice, even the best clocks have some long-term instabilities associated with them. As mentioned in Section III, these long-term clock instabilities correspond to the frequency drift terms of the oscillators. If these frequency drift terms are

slowly varying, i.e., the time constants of the drifts are much greater than the time constants of the network, then the steady-state results obtained in the previous sections are still valid. So, for the case of slowly varying clock frequencies, the steady-state results can be obtained by simply replacing the constant frequencies in the equations with the time-varying frequencies. For example, in the case of fully connected mutually synchronized networks with delay line compensation, the steady-state time error between the nodes is given in Table 4. If slowly varying clock frequencies are assumed for this case, the steady-state time error is given by

$$T_{ri}(t) = \frac{N-1}{N} \frac{\Omega_r(t) - \Omega_i(t)}{B}$$

$$- \frac{1}{N} \Omega_s(t) \left[\sum_{\substack{j=1 \\ j \neq r}}^{N} \Delta\tau_{rj} - \sum_{\substack{j=1 \\ j \neq 1}}^{N} \Delta\tau_{ij} \right]. \quad (86)$$

Assuming that the delays are fully compensated in this network, i.e., $\Delta\tau_{ij} = 0$, $\forall i, j$, and substituting for the free-running frequencies of the clocks from (15), gives the steady-state time error

$$T_{ri}(t) = \frac{N-1}{N} \frac{1}{B} \sum_{k=1}^{M} \frac{q_{ri}(k)}{(k-1)!} t^{k-1} \quad (87)$$

where

$$q_{ri}(k) = q_r(k) - q_i(k). \quad (88)$$

For comparison purposes the time error buildup in a plesiochronous network can be found from (13), and is given by (short-term instabilities neglected)

$$T_{ri}(t) = \sum_{k=1}^{M} \frac{q_{ri}(k)}{k!} t^k. \quad (89)$$

Comparing (88) and (89), it can be seen that by mutually synchronizing the network, the rate of increase in the time error between the nodes has been slowed considerably. This is the main advantage of synchronous networks over plesiochronous networks. From (87), it is clear that by increasing the loop gain B, the time error between the nodes is reduced. However, the maximum allowable value of B is determined from the stability condition of the network given in Section V.

VIII. Influence of Clock Phase Noise

The mathematical model of the clock given in (12) indicates that the time process of each clock depends on the short-term clock instabilities $\Psi(t)$. Although the process $\Psi(t)$ is in general a nonstationary stochastic process, $\dot{\Psi}(t)$ can be assumed to be stationary [89].

Since the time process $T(t)$ given by (12) is a nonstationary random process, its behavior cannot be characterized in terms of power spectral density. However, the nth increment ($n \geq M$) of $T(t)$ is a stationary process and can be used as a measure of performance of the clock. Thus the performance of the network can be characterized in terms of the nth increment of the time processes observed at the network nodes, the time error generated between them, and their associated structure functions. The time error process and its first increment, the time interval error process, were defined in Section IV. Similarly, one can define the higher increments of the time error process. The nth increment of the time error process, for $n > 1$, is defined recursively by [89]

$$\Delta^n T_{ij}(t; h) = \Delta^{n-1} \left[\Delta T_{ij}(t; h) \right]. \quad (90)$$

The process $T_{ij}(t)$ is called a process with stationary nth increment if $\Delta^n T_{ij}(t; h)$ is a stationary process. The nth structure function of a process $T_{ij}(t)$ with stationary nth increment is defined by

$$D^n_{T_{ij}}(h) \triangleq E\left[\Delta^n T_{ij}(t; h) \right]^2 \quad (91)$$

which is basically the variance of the nth-increment process and can be related to the power spectral density of the appropriate interval process through

$$D^n_{T_{ij}}(h) = \int_{-\infty}^{\infty} S_{\Delta^n T_{ij}}(\omega) \frac{d\omega}{2\pi}. \quad (92)$$

In a similar manner one can define the nth increment and hence the nth-structure function of the time processes observed at the network nodes by

$$D^n_{T_i}(h) = E\left[\Delta^n T_i(t; h) \right]^2 = \int_{-\infty}^{\infty} S_{\Delta^n T_i}(\omega) \frac{d\omega}{2\pi}. \quad (93)$$

$D^n_{T_i}(h)$ and $D^n_{T_{ij}}(h)$ have been calculated for plesiochronous, master–slave, and mutually synchronized networks of clocks [87], [92], and the results are tabulated in Tables 6 and 7,

Table 6 The nth Structure Function of the Time Processes Generated at Network Nodes

Plesiochronous Network

$$D^n_{T_i}(h) = 2^{2n} \int_{-\infty}^{\infty} \sin^{2n}\left(\frac{\omega h}{2} \right) \frac{S_{\Psi_i}(\omega)}{2} \frac{d\omega}{2\pi}$$

Master–Slave Network

$$D^n_{T_i}(h) = 2^{2n} \int_{-\infty}^{\infty} \sin^{2n}\left(\frac{\omega h}{2} \right) |G_{ms}(\omega)|^2 \frac{S_{\Psi_i}(\omega)}{\omega^2} \frac{d\omega}{2\pi}$$

$$|G_{ms}(\omega)|^2 = |H(\omega)|^{2(L-1)} + \sum_{k=0}^{L-2} |H(\omega)|^{2K} \cdot |1 - H(\omega)|^2$$

Mutually Synchronized Network

$$D^n_{T_i}(h) = 2^{2n} \int_{-\infty}^{\infty} \sin^{2n}\left(\frac{\omega h}{2} \right) |G_{mu}(\omega)|^2 \frac{S_{\Psi_i}(\omega)}{\omega^2} \frac{d\omega}{2\pi}$$

$$|G_{mj}(\omega)|^2 = \frac{|(N-1) - (N-2)H(\omega)e^{-j\omega\tau} + (N-1)|H(\omega)|^2}{|(N-1) + H(\omega)e^{-j\omega\tau}|^2 |1 - H(\omega)e^{-j\omega\tau}|^2} |1 - H(\omega)|^2$$

Table 7 The nth Structure Function of the Time Error Process Generated Between Network Nodes

Plesiochronous Network

$$D_{T_{ij}}^n(h) = 2^{2n} \int_{-\infty}^{\infty} \sin^{2n}\left(\frac{\omega h}{2}\right) \frac{S_{\psi_{ij}}(\omega)}{\omega^2} \frac{d\omega}{2\pi}$$

Master–Slave Network

$$D_{T_{ij}}^n(h) = 2^{2n} \int_{-\infty}^{\infty} \sin^{2n}(\frac{\omega h}{2})|H_{ms}(\omega)|^2 \frac{S_{\psi_{ij}}(\omega)}{\omega^2} \frac{d\omega}{2\pi}$$

$$|H_{ms}(\omega)|^2 = \frac{1}{2}\left\{1 + |H(\omega)|^{2(L-1)} + \sum_{k=0}^{L-2}|H(\omega)|^{2k}|1 - H(\omega)|^2\right\} - \text{Re}\left\{[H^*(\omega)e^{j\omega\tau}]^{L-1}\right\}$$

Mutually Synchronized Network

$$D_{T_{ij}}^n(h) = 2^{2n} \int_{-\infty}^{\infty} \sin^{2n}\left(\frac{\omega h}{2}\right)|H_{mu}(\omega)|^2 \frac{S_{\psi_{ij}}(\omega)}{\omega^2} \frac{d\omega}{2\pi}$$

$$|H_{mu}(\omega)|^2 = \frac{|(N-1) - (N-2)H(\omega)e^{-j\omega\tau}|^2 + (2N-3)|H(\omega)|^2 - 2(N-1)\text{Re}\left\{H(\omega)e^{-j\omega\tau}\right\}}{|(N-1) + H(\omega)e^{-j\omega\tau}|^2 \cdot |1 - H(\omega)e^{-j\omega\tau}|^2}|1 - H(\omega)|^2$$

where

$$H(s) = \frac{BF(s)}{s + BF(s)} \qquad (94)$$

with

$$F(s) = \frac{1}{1 + Ts} \qquad (95)$$

is the loop transfer function, L is the level of the clock in the hierarchy, N is the number of clocks in the fully connected mutually synchronized network, and τ is the delay between the clocks which is assumed to be the same between all clocks.

From the results presented in these tables it can be seen that the master–slave and mutual synchronization techniques have the effect of filtering the clock phase noise processes by some fitler function. For the case where the effect of phase noise on the time processes of the nodal clocks is considered, the filter function introduced by mutual synchronization is $G_{mu}(\omega)$ with a frequency response as shown in Fig. 19 and the frequency response of the filter introduced by master–slave synchronization $G_{ms}(\omega)$ is shown in Fig. 20. These figures indicate that as far as the
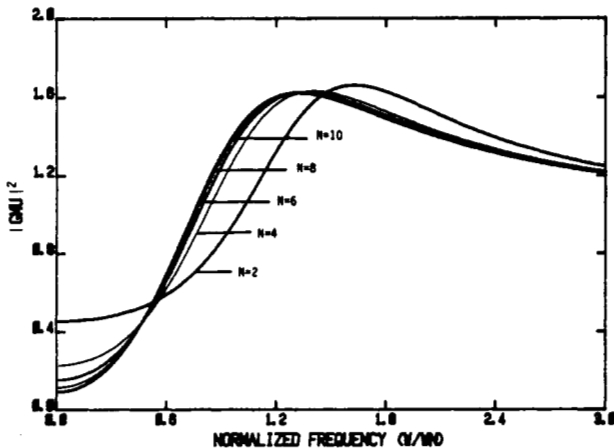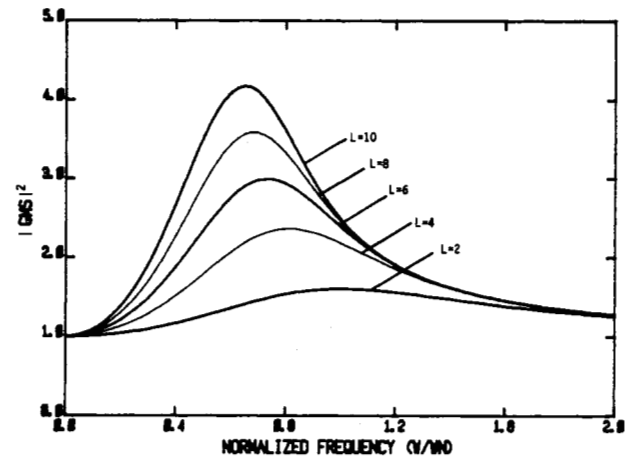
Fig. 20. Frequency response of the nodal filtering function for master–slave synchronized network.

effect of phase noise on the time processes of the clocks is concerned, the performance of the master–slave networks is inferior to that of plesiochronous networks, while better performance can be seen in mutually synchronized networks. Moreover, as the number of levels in the hierarchy increases, the effect of phase noise becomes more significant, whereas as the number of nodes in the mutually synchronized network increases the effect of phase noise is reduced.

For the case where the effect of phase noise on the time error processes between the clocks of the network is being considered, the filter function introduced by mutual synchronization is $H_{mu}(\omega)$ whose frequency response is depicted in Fig. 21, and the filter function introduced by the master–slave synchronization is $H_{ms}(\omega)$ whose frequency response is shown in Fig. 22. From these figures it can be seen that mutual synchronization results in the reduction of the effect of phase noise on the time error processes, especially in low-frequency regions where this reduction is of particular importance because of $1/f$-type spectrum of the phase noise processes. This reduction becomes more significant as the number of nodes in the network N increases. Master–slave synchronization also results in the
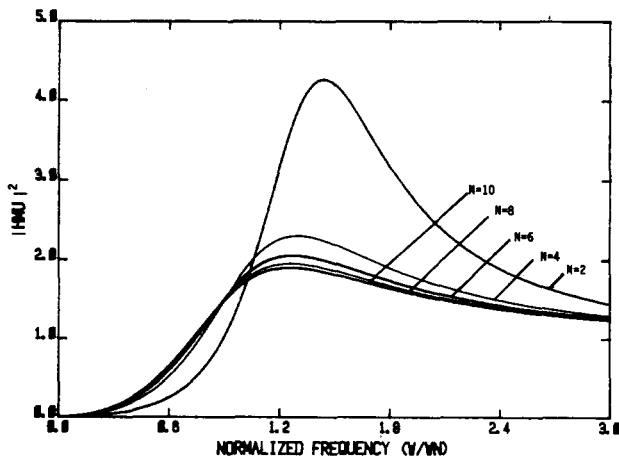
Fig. 19. Frequency response of the nodal filtering function for mutually synchronized network.

Fig. 21. Frequency response of the time error filter function for mutually synchronized network.
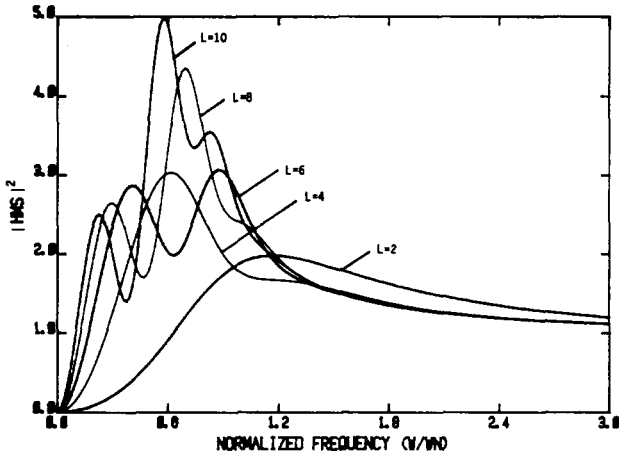

Fig. 22. Frequency response of the time error filter function for master–slave synchronization technique.

reduction of the effect of phase noise at low frequencies, however, this technique increases the effect of phase noise at other frequencies. Thus master–slave synchronization can improve or degrade the performance of the network depending on the spectrum of the phase noise, the loop gain at each node, and the level of the node in the hierarchy.

IX. SYNCHRONIZATION BEHAVIOR IN THE PRESENCE OF CHANNEL NOISE

As mentioned earlier, it may be convenient to ignore the channel thermal noise when it is desired to obtain fairly simple estimates of the synchronization performance under somewhat idealized conditions. This has been done, for example, in Sections V and VI. Although the presence of channel noise complicates the behavior of synchronization networks, no complete understanding of the process of synchronization may be gained without analyzing the random effects of thermal noise.

The mathematical model developed for synchronization networks in Section III accounts for thermal noise. The solution of (28) in its most general form and in the presence of channel noises is a formidable, if not impossible, task. Equation (28) is in general a set of N coupled nonlinear stochastic differential equations. The key to studying the

behavior of the network in the presence of thermal noise is to begin by simplifying the network topology as much as possible. This means studying a network consisting of two nodes only. After the results are developed and understood for that case, the trends that occur with increasing the nodes from two to N are predicted.

Plesiochronous networks are naturally unaffected by channel thermal noise. This is true since no information is transmitted between the nodes. Master–slave and mutually synchronized networks are treated using the same approach based on phase-lock loop (PLL) theory. The development here will concentrate on the simplest of the statistical performance measures, viz., the phase error between nodes. This is because it is the least difficult to obtain and explain. The development for a pair of mutually synchronized nodes is somewhat more general than for a pair of master–slave nodes and will be outlined first. The results for the master–slave case will then be given and the two performances compared.

Assuming a first-order PLL (no loop filter) for the configuration of Fig. 9, we can write the equations of operation of the two PLLs in terms of the phase processes and thermal noise as follows[1] [81]:

$$\frac{d\Phi_1(t)}{dt} = \omega_{01} + A_1 B_1 \sin\left[\Phi_2(t - \tau_{12})\right.$$
$$\left. - \Phi_1(t - \hat{\tau}_{12})\right] + B_1 n_1(t) \quad (96a)$$

$$\frac{d\Phi_2(t)}{dt} = \omega_{02} + A_2 B_2 \sin\left[\Phi_1(t - \tau_{21})\right.$$
$$\left. - \Phi_2(t - \hat{\tau}_{21})\right] + B_2 n_2(t) \quad (96b)$$

where

ω_{0i} free-running frequency of oscillator i, $i = 1, 2$.

A_i open-loop gain of PLL i; $i = 1, 2$.

$A_i B_i$ closed-loop gain of PLL i; $i = 1, 2$.

$\Phi_i(t)$ phase process at output of oscillator i; $i = 1, 2$. This is the phase of the sinusoidal oscillation at the output of the ith oscillator at time t.

$n_i(t)$ equivalent phase noise process for PLL i [81]; it is white Gaussian with $N_0/2$ power spectral density.[2]

Here the phase characteristics of the PLLs are assumed to have their inherently sinusoidal nature. Also, it is assumed that the system is observed over a period during which the long-term clock drifts can be neglected. With today's technology these periods can be as long as hours, days, or longer. The system is assumed to reach a steady state in which a steady-state frequency process $\omega_s(t)$ is sustained at the output of the two oscillators [82], [91]. The instantaneous fluctuations in $\omega_s(t)$ are due to the noise in the system and therefore $\omega_s(t)$ can be assumed first-order stationary. This means that it has a constant time-independent mean $\bar{\omega}$. This leads to the steady-state approximation [82]

$$\Phi_i(t + \tau_{ij}) \approx \Phi_i(t) + \tau_{ij}\bar{\omega}. \quad (97)$$

Subtracting (96a) from (96b) and using (97) gives (when $A_1 = A_2 = A$ and $B_1 = B_2 = B$)

[1]The notation followed here is slightly different from the notation used in (22) but is more in agreement with that used in the literature on this topic.

[2]The reader unfamiliar with the theory of PLLs is advised to consult [81] for a comprehensive description of the signal and noise processes in a PLL.

$$\frac{d\Delta\Phi_{21}(t)}{dt} = (\omega_2 - \omega_1) - 2AB\cos(\psi_e)$$

$$\cdot \sin[\Delta\Phi_{21}(t) + \theta_e] - \sqrt{2}\,Bn(t) \quad (98)$$

where

$$\psi_e = \bar{\omega}(\Delta\tau_{21} + \Delta\tau_{12})/2 \quad (99)$$

$$\theta_e = \bar{\omega}(\Delta\tau_{21} - \Delta\tau_{12})/2 \quad (100)$$

and as previously defined $\Delta\tau_{ij} = \tau_{ij} - \hat{\tau}_{ij}$.

Equation (98) is the key stochastic differential equation describing the phase error $\Delta\Phi_{21}$. Its solution resembles the solution of the differential equation describing the phase error in a sinusoidal PLL [81]. $\Delta\phi_{21}(t)$ is first defined to be the mod-2π reduction of $\Delta\Phi_{21}(t)$ about $(2n \pm 1)\pi$. The solution of the Fokker–Planck equation associated with (98) gives in the steady state (t dropped) for $\Delta\phi_{21}\epsilon[(2n-1)\pi, (2n+1)\pi]$ and any integer n [91]

$$p(\Delta\phi_{21}) = \frac{\exp[\beta_{21}\Delta\phi_{21} + \alpha\cos(\Delta\phi_{21} + \theta_e)]}{4\pi^2|I_{j\beta_{21}}(\alpha)|^2 \exp(-\pi\beta_{21})}$$

$$\cdot \int_{y=\Delta\phi_{21}}^{\Delta\phi_{21}+2\pi} \exp\{-[\beta_{21}y + \alpha\cos(y + \theta_e)]\}\,dy \quad (101)$$

where $p(\Delta\phi_{21})$ is the probability density function (pdf) of $\Delta\phi_{21}$ and

$$\alpha = \rho\cos\psi_e \quad (102)$$

$$\beta_{21} = 2(\omega_2 - \omega_1)/B^2 N_0 \quad (103)$$

with

$$\rho = 4A/BN_0. \quad (104)$$

ρ is the familiar signal-to-noise ratio (SNR) in the loop bandwidth [81]. α is the effective SNR for the mutually synchronized nodes. It depends on the residual delays. β_{21}

is the normalized frequency detuning between the two oscillators.

The effects of residual delays on the density of the phase error between the two mutually synchronized oscillators is shown in Fig. 23. The effects of residual delays are manifested in two ways:

1) The effective SNR is reduced. If ψ_e increases from its ideal value of zero to $\pi/2$, α drops from its maximum value of ρ to zero. This causes the flattening of $p(\Delta\phi_{12})$. It implies an increased uncertainty in the phase error, and an increase in the probability of losing synchronization due to cycle slipping [91]. Here cycle slipping refers to a slip by one oscillator relative to the other.

2) If the residual delays in the two directions are not equal, i.e., $\Delta\tau_{12} \neq \Delta\tau_{21}$, $p(\Delta\phi_{21})$ is shifted to a nonzero mean θ_e. If this timing bias is known it can be calibrated out. If, however, it varies slowly with time, as it inevitably will, there will be an unknown bias error in the time difference between the two nodes.

The effect of β_{21} on $p(\Delta\phi_{21})$ is similar to the effect of detuning on a sinusoidal PLL [81]. β_{21} causes $p(\Delta\phi_{21})$ to be asymmetric about zero and introduces a nonzero mean into it.

For a pair of nodes synchronized in the master–slave mode (Fig. 7), the equation for the master node may be written as $d\Phi_m(t)/dt = \omega_m$ (the subscript m denotes the master, the subscript s will denote the slave). Subtracting this from the equation of the slave PLL gives the following equation for the phase error between the master and the slave:

$$\frac{d\Delta\Phi_{ms}(t)}{dt} = (\omega_m - \omega_s) - A_s B_s$$

$$\cdot \sin[\Delta\Phi_{ms}(t) - \bar{\omega}\Delta\tau_{sm}] - B_s n_s(t). \quad (105)$$
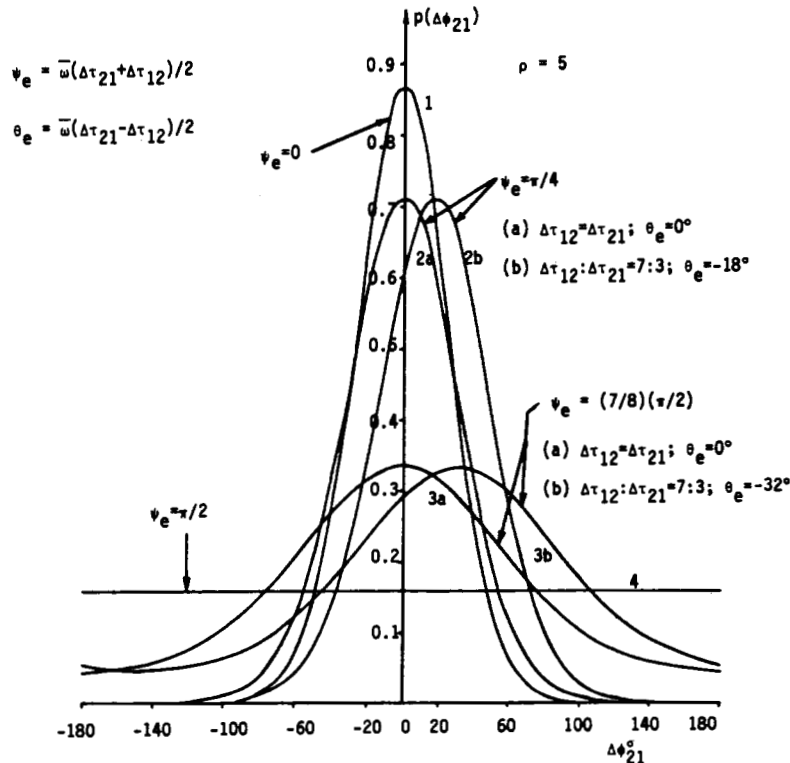
Equation (105) leads to a solution very similar in form to

Fig. 23. The effect of residual delays on the probability density function $p(\Delta\phi_{21})$ of the phase error in a two-nodal mutually synchronized network.

(101). There are some differences, however, that can be seen by comparing (105) and (98).

1) The factor $\cos(\psi_e)$ multiplying $\sin[\cdot]$ is absent in (105). This means that $p(\Delta\phi_{21})$ for the master–slave case does not exhibit a reduction in effective SNR due to nonzero residual delays, i.e., for the master–slave case $\alpha = \rho$.

2) $\bar{\omega}\Delta\tau_{sm}$ in (105) replaces $\theta_e = \bar{\omega}(\Delta\tau_{21} - \Delta\tau_{12})/2$. This indicates that for the master–slave case there is an increase in the dependence of the bias shift in $p(\Delta\phi_{21})$ on the residual delays. This is because $\Delta\tau_{21}$ and $\Delta\tau_{12}$ will tend to cancel out. If the residual delays are viewed as random variables (very slowly varying processes compared to the thermal noise) the mean of θ_e will be proportional to the difference of the means of the two residual delays, while $\bar{\omega}\Delta\tau_{sm}$ will have a mean proportional to that of $\Delta\tau_{sm}$. Moreover, the variance of θ_e will be half the variance of $\bar{\omega}\Delta\tau_{sm}$.

3) The constant coefficients in (98) are different from those in (105). The coefficients in (105) yield a normalized detuning $\beta_{ms} = 4(\omega_m - \omega_s)/B^2N_0$. Comparing this value to β_{21} in (103) shows that the master–slave is twice as sensitive to detuning as the mutual configuration.

The density function of $\Delta\phi_{21}$ resulting from (105) is similar to (101) except for the replacement of β_{21} by β_{ms}, using $\alpha = \rho$, and replacing ψ_e by $\bar{\omega}\Delta\tau_{sm}$. The effects of combined detuning and residual delays on the densities of the phase error are compared in Fig. 24 for the mutual and master–slave cases.

As clearly seen from Figs. 23 and 24 the thermal noise causes the spread in the density of the phase error about its mean. It would be thus expected that for very high SNR the value of the phase error will be the mean value of its

density. This is indeed true. First, at high SNR, the curve for $p(\Delta\phi_{21})$ becomes very close to a Gaussian curve. $p(\Delta\phi_{21})$ is closely approximated by a Gaussian density of mean $(\beta_{21}/\rho) - \theta_e$ for mutual synchronization [91]. This is similar to the behavior of the phase error in a single PLL at high SNR [81]. For master–slave, the mean phase error is $\beta_{ms}/\rho - \bar{\omega}\Delta\tau_{sm}$. For both cases, the variance is approximately $1/\rho$ (provided the residual delays are not too large for the mutual case). It is very interesting to note that these means agree with the values of the timing errors predicted in the absence of noise. This is seen from the second entry in Tables 4 and 5 when the SNR is sufficiently high.

At moderate and lower SNRs, the network with N nodes is much harder to analyze. This problem has been addressed in [90] and [103]. It is concluded that for mutual synchronization the timing bias errors between each two connected nodes depends on the average of the residual delays throughout the network. The expected values of the phase or timing errors average out in a way similar to that shown in the second entry of Tables 4 and 5 provided that the residual delays are small. A more detailed exposition of the deleterious effects of noise and residual delays in N-nodal networks is beyond the scope of this tutorial review.

Other work aiming at a more complete understanding of the synchronization behavior in the presence of thermal noise has also been performed. The random nature of the nodal time scales and the time interval errors described in Section IV by the statistical performance measures (b) and (c), respectively, have been characterized [82], [91]. Random oscillator frequency instability effects have been studied, also useful Gaussian approximations to the densities de-
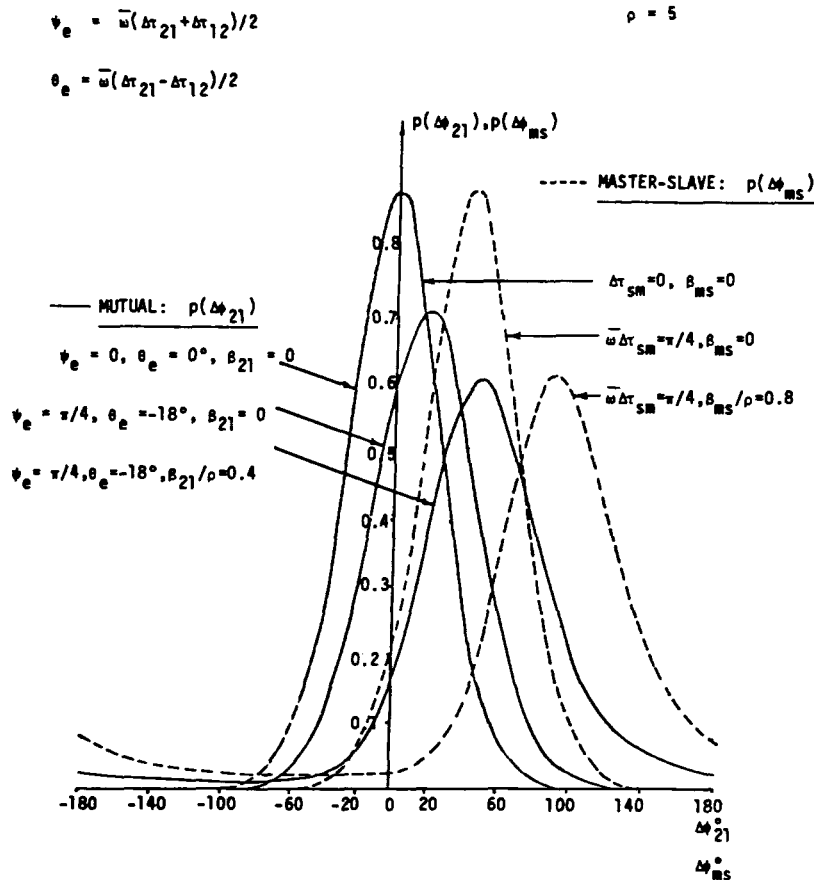

Fig. 24. Comparison of the combined effects of the residual delays and detuning on the probability density functions of the phase error in mutual and master–slave synchronization.

scribing the nodal time intervals and time interval errors have been developed. The interested reader is referred to [82] and [91] for these results.

REFERENCES

[1] J. Buck and E. Buck, "Synchronous fireflies," *Scient. Amer.*, May 1976.

[2] R. S. Graham, "Pulse transmission systems," U.S. Patent 3 042 751, submitted July 3, 1962.

[3] J. S. Mayo, "PCM network synchronization," U.S. Patent 3 136 861, submitted 1964.

[4] _____, "Experimental 224 Mb/s PCM terminals," *Bell Syst. Tech. J.*, vol. 44, pp. 1813–1841, Nov. 1965.

[5] _____, "Synchronization of PCM networks," in *IEEE NEREM Rec.*, vol. 7, p. 166, 1965.

[6] _____, "Theory for some asynchronous time division switches," *Bell Syst. Tech. J.*, vol. 50, May–June 1971.

[7] F. K. Fultz and D. B. Perrick, "The TI carrier system," *Bell Syst. Tech. J.*, vol. 44, pp. 1405–1486, Sept. 1965.

[8] F. J. Witt, "An experimental 224 Mb/s digital multiplexer-demultiplexer using pulse stuffing synchronization, *Bell Syst. Tech. J.*, vol. 44, pp. 1843–1885, Nov. 1965.

[9] V. I. Johannes and R. H. McCollougt, "Multiplexing of asynchronous digital signals using pulse stuffing with added-bit signalling," *IEEE Trans. Commun. Technol.*, vol. COM-14, no. 5, pp. 562–568, Oct. 1966.

[10] S. Butmann, "Synchronization of PCM channels by method of word stuffing," *IEEE Trans. Commun. Technol.*, vol. COM-16, no. 2, pp. 252–254, Apr. 1968.

[11] R. A. Bruce, "1.5 to 6M bit digital mux employing pulse stuffing," in *Proc. Int. Conf. on Commun.*, June 1969.

[12] M. M. Buchner, Jr., "An asymmetric encoding scheme for word stuffing," *Bell Syst. Tech. J.*, vol. 49, no. 3, pp. 379–398, March 1970.

[13] W. Fleig, "Stuffing TDM for independent TI bit streams," *Telecommun.*, vol. 6, no. 7, pp. 23–32, July 1972.

[14] Y. Matsura, S. Kozuka, and K. Yuki, "Jitter characteristics of pulse stuffing synchronization," in *Proc. Int. Conf. on Commun.*, pp. 259–264, June 1968.

[15] P. E. K. Chow, "Jitter due to pulse stuffing synchronization," *IEEE Trans. Commun.*, vol. COM-21, pp. 854–859, July 1973.

[16] H. A. Stover, "Communication network timing," Defense Comm. Eng. Center, Tech. Rep. TR 43-75, AD-A021934, Sept. 1975.

[17] _____, "Timing and synchronization of switched digital communication networks," in *Proc. ICC '76*, pp. 25.1–25.6, June 1976.

[18] _____, "Improved time reference distribution for a synchronous digital communications network," in *Proc. 8th Annual Precise Time and Time Interval (PTTI) Applications and Planning Meet.* (U.S. Naval Res. Cen., Nov. 1976), pp. 147–166.

[19] _____, "Suggested attributes for timing in a digital DCS," in *Proc. 11th Annual Precise Time and Time Interval (PTTI) Application and Planning Meet.* (U.S. Naval Res. Cen.), 1979.

[20] _____, "Network timing/synchronization for defense communications," *IEEE Trans. Commun.*, vol. COM-28, pp. 1234–1244, Aug. 1980.

[21] E. A. Harrington, "Synchronization techniques for various switching network topologies," *IEEE Trans. Commun.*, vol. COM-26, pp. 925–932, June 1978.

[22] CCITT, "Plesiochronous operation of international digital links," *Recommendation G.812*, vol. III-2, pp. 25–10/15.

[23] G. P. Darwin and R. C. Prim, "Synchronization in a system of interconnected units," U.S. Patent 2 986 723, filed Feb. 26, 1960.

[24] T. Eqawa, M. Makimo, and Y. Inouse, "A study on master-slave synchronization technique," in *Proc. Int. Switching Symp.* (Kyoto, Japan, 1976), pp. 441-3-1/8.

[25] J. E. Cox, "Western Union digital services," *Proc. IEEE*, vol. 60, pp. 854–859, Nov. 1972.

[26] A. R. Worley, "The Datran system," *Proc. IEEE*, vol. 60, pp. 1357–1368, Nov. 1972.

[27] B. R. Saltzberg and H. M. Zydney, "Digital data system: Network synchronization," *Bell Syst. Tech. J.*, vol. 54, no. 5, pp. 879–892, May–June 1975.

[28] L. H. Brandenburg, "Timekeeping in the Bell System switched digital network," in *Proc. Int. Conf. on Commun.*, pp.

[29] 25–26/29, June 1976.

[29] M. Decina, A. Pietromarchi, A. Bovo, and L. Musumeci, "Development of network synchronization techniques in Italy," in *Proc. Int. Conf. on Commun.*, pp. 21–25/25, June 1976.

[30] J. E. Abate, L. H. Branceeberg, J. C. Lawson, and W. L. Ross, "The switched digital network plan," *Bell Syst. Tech. J.*, vol. 56, no. 7, pp. 1297–1320, Sept. 1977.

[31] R. G. Dewitt, "Network synchronization plan for Western Union all digital network," *Telecommun.*, pp. 25–28, July 1973.

[32] F. T. Chen, H. Goto, and O. G. Gabbard, "Timing synchronization of Datran digital data network," in *Proc. Nat. Telecomm. Conf.*, 1975.

[33] F. A. Mitchell and R. A. Boulter, "Synchronization of the digital network in United Kingdom," in *Proc. Int. Conf. on Commun.* (Boston, MA, 1979), pp. 11.2.1/4.

[34] V. E. Benes, "A method of controlling the frequencies of timing signals by phase averaging and comparison," unpublished Bell Telephone Laboratories memorandom, Murry Hill, NJ, Sept. 1959.

[35] J. P. Runyon, "Reciprocal timing of time division switching centers," U.S. Patent 3 050 585, filed May 20, 1960.

[36] M. B. Brilliant, "The determination of frequency in systems of mutually synchronized oscillators," *Bell Syst. Tech. J.*, vol. 45, pp. 1737–1748, Dec. 1966.

[37] _____, "Dynamic response of systems of mutually synchronized oscillators," *Bell Syst. Tech. J.*, vol. 46, pp. 319–356, Feb. 1967.

[38] M. Karnaugh, "A model for organic synchronization of communication systems," *Bell Syst. Tech. J.*, vol. 45, pp. 1705–1735, Dec. 1966.

[39] A. Gersho and B. J. Karafin, "Mutual synchronization of geographically separated oscillators," *Bell Syst. Tech. J.*, vol. 45, pp. 1689–1704, Dec. 1966.

[40] H. Inose, H. Fujisaki, and T. Saito, "Theory of mutually synchronized systems," *Electron. Commun. in Japan*, vol. 49, no. 4, pp. 263–271, Apr. 1966.

[41] H. Inose, T. Saito, P. V. Thinh, and S. Sakata, "Consideration on CPM integrated communication system including mobile terminals with particular reference to synchronization," in *Proc. Int. Switching Symp.* (Munich, FRG, Sept. 9–13, 1974), pp. 221/1-221/7.

[42] R. H. Bosworth, F. W. Kammerer, D. E. Rowlinson, and J. V. Scattaglia, "Design of a simulator for investigating organic synchronization systems," *Bell Syst. Tech. J.*, vol. 47, pp. 209–226, Feb. 1968.

[43] J. C. Candy and M. Karnaugh, "Organic synchronization: Design of the controls and some simulation results," *Bell Syst. Tech. J.*, vol. 47, pp. 227–259, Feb. 1968.

[44] J. R. Pierce, "Synchronizing digital networks," *Bell Syst. Tech. J.*, vol. 48, no. 3, pp. 615–636, Mar. 1969.

[45] _____, "Network for block switching of data," *Bell Syst. Tech. J.*, vol. 51, no. 6, pp. 1133–1145, July–Aug. 1972.

[46] I. W. Sandberg, "On conditions under which it is possible to synchronize digital transmission systems," *Bell Syst. Tech. J.*, vol. 48, pp. 1999–2022, July–Aug. 1969.

[47] _____, "Some properties of a nonlinear model of a system for synchronizing digital transmission networks," *Bell Syst. Tech. J.*, vol. 48, pp. 2975–2997, Nov. 1969.

[48] M. W. Willard, "Analysis of a system of mutually synchronized oscillators," *IEEE Trans. Commun. Technol.*, vol. COM-18, no. 5, pp. 467–483, Oct. 1970.

[49] M. W. Willard and H. R. Dean, "Dynamic behavior of a system of mutually synchronized oscillators," *IEEE Trans. Commun. Technol.*, vol. COM-19, no. 4, pp. 373–395, Aug. 1971.

[50] J. P. Morland, "Performance of a system of mutually synchronized clocks," *Bell Syst. Tech. J.*, vol. 50, no. 7, pp. 2249–2464, Sept. 1971.

[51] R. F. E. Dell, "Features of a proposed synchronous data network," *IEEE Trans. Commun.*, vol. COM-20, no. 3, p. 499, June 1972.

[52] R. W. Chang, "Analysis of a dual mode digital synchronization system employing digital rate locked loops," *Bell Syst. Tech. J.*, vol. 51, no. 8, pp. 1881–1911, Oct. 1972.

[53] R. H. Bittel, W. B. Elsner, H. Helm, R. Mukundan, and D. A. Perreault, "Clock synchronization through discrete control connection," *IEEE Trans. Commun.*, vol. COM-22, no. 6, pp.

836–839, June 1974.

[54] A. C. Davies, "The effect of clock drift upon the synchronization of digital communication networks," *IEEE Trans. Commun.*, vol. COM-22, no. 11, pp. 1842–1844, Nov. 1974.

[55] ———, "Discrete-time synchronization of digital data networks," *IEEE Trans. Circuits Syst.*, vol. CAS-22, no. 7, pp. 610–618, July 1975.

[56] R. Ishii, "Dynamic response and stability of mutually synchronized systems," *IEEE Trans. Commun.*, vol. COM-23, No. 4, pp. 443–448, Apr. 1975.

[57] J. Yamato, S. Nakajima, and K. Saito, "Dynamic behavior of a synchronized control system for an integrated telephone network," *IEEE Trans. Commun.*, vol. COM-22, no. 6, pp. 839–845, June 1974.

[58] J. Yamato, "Stability of a synchronization control for an integrated telephone network," *IEEE Trans. Commun.*, vol. COM-22, no. 11, pp. 1848–1853, Nov. 1974.

[59] J. Yamato, M. Ono, and S. Usuda, "Synchronization of a PCM integrated telephone network," *IEEE Trans. Commun. Technol.*, vol. COM-16, no. 1, pp. 1–11, Feb. 1968.

[60] H. L. Hartmann, "Simulationsverzuch zur Synchronisierung Integrierter PCM-Netze," *Frequenz*, vol. 22, no. 1, pp. 28–29, 1968.

[61] ———, "Synchronisierung Integrierter PCM-Netze durch Digital-gesteuerte Phasenmittelung," *Nachrichtentech. Z.*, vol. 21, no. 9, pp. 533–539, 1968.

[62] ———, "Merkmale Digitaler Asynchron oder Synchron Arbeitender Informationsnetze mit hoher Bitrate," *Nachrichtentech. Z.*, vol. 23, no. 6, pp. 302–307, 1970.

[63] ———, "The single ended principle of digitally controlled phase averaging for the synchronization of communication networks," *Nachrichtentech. Z.*, vol. 28, no. 12, pp. 421–426, 1975.

[64] ———, "Time and frequency instability of communication networks," in *Proc. NTC 1981* (New Orleans, LA), pp. F1.1.1–F1.1.7.

[65] A. Darre and C. Karl, "Theorie and Simulation eines Synchronisierten PCM Netzes vol Oszillatoren mit Geyenseitiger Synchronisation," *Nachrichtentech. Z.*, vol. 23, no. 5, pp. 257–261, 1970.

[66] A. Darre, "Der Einfluss der Laufzeiten auf den Synchronisierungsvorgang in einem PCM Netz," *Nachrichtentech. Z.*, vol. 23, no. 11, pp. 558–560, 1970.

[67] O. Karl, "Synchronisierverfahren von Integrierter PCM-Netzen nach dem Phasenmittelungsprinzip," *Nachrichtentech. Z.*, vol. 23, no. 8, pp. 470–411, 1970.

[68] E. Mitwally, "A control system for clocks where mutual synchronization being the main mode of operation," Rep. TRITA-TTS-7403, Royal Inst. Technol., Stockholm, Sweden, Dec. 1974.

[69] A. Datta and E. Mitwally, "Synchronization of multi-exchange local network by bit-by-bit method," *IEEE Trans. Commun.*, vol. COM-27, no. 7, pp. 1034–1046, 1979.

[70] A. Marlevi, "Direct digitally controlled network synchronization," *IEEE Trans. Commun.*, vol. COM-27, no. 10, pp. 1561–1565, 1979.

[71] ———, "An effective set of network synchronization methods: General considerations and practice," in *Proc. ICC 82* (Philadelphia, PA), pp. 5H.1.1–5H.1.6.

[72] H. Mumford and P. W. Smith, "Synchronization of a PCM network using digital techniques," *Proc. IEEE*, vol. 54, pp. 1420–1428, Sept. 1966.

[73] N. West, "Synchronous digit switching in highly interconnected communication networks," *Proc. IEEE*, vol. 55, pp. 1378–1384, Oct. 1967.

[74] W. C. Lindsey and A. V. Kantak, "Synchronization by means of master slave returnable timing system," in *Proc. Int. Telemetry Conf.*, 1979.

[75] ———, "Network synchronization by means of returnable timing system," *IEEE Trans. Commun.*, vol. COM-26, no. 6, pp. 892–896, June 1978.

[76] W. C. Lindsey, A. V. Kantak, and A. Dobrogovski, "Mutual synchronization properties of a system of two oscillators with sinusoidal phase detectors," *IEEE Trans. Commun.*, vol. COM-24, no. 12, pp. 1321–1326, Dec. 1976.

[77] W. C. Lindsey and A. V. Kantak, "Mathematical model for time transfer networks," in *Proc. Int. Conf. on Commun.*, (Toronto, Ont., Canada, June 1978).

[78] ———, "Network synchronization of random signals," *IEEE Trans. Commun.*, vol. COM-28, no. 8, pp. 1245–1259, Aug. 1980.

[79] W. C. Hagmann and W. C. Lindsey, "Network synchronization techniques," in *Proc. NATO ASI* (Norwich, England, Aug. 1980).

[80] W. C. Hagmann, F. Ghazvinian, and W. C. Lindsey, "Synchronization techniques for mobile user satellite systems," in *Proc. Int. Conf. on Commun.* (Denver, CO, June 1980).

[81] W. C. Lindsey, *Synchronization Systems in Communication and Control.* Englewood Cliffs, NJ: Prentice-Hall, 1972.

[82] K. Dessouky and W. C. Lindsey, "Phase and frequency transfer between mutually synchronized oscillators," *IEEE Trans. Commun.*, vol. COM-32, no. 2, pp. 110–117, Feb. 1984.

[83] W. C. Lindsey and H. J. Choi, "Mutual synchronization of two oscillators," presented at NTC 82, Galveston, TX, Nov. 1982.

[84] K. Dessouky and W. C. Lindsey, "Statistical characterization of a system of two mutually synchronized oscillators," presented at NTC 82, Galveston, TX, Nov. 1982.

[85] W. C. Lindsey and F. Ghazvinian, "Dissemination of time in a digital communication network," presented at the Nat. Radio Sci. Meet., Boulder, CO, Jan. 1981.

[86] W. C. Lindsey, F. Ghazvinian, and W. C. Hagmann, "Time and frequency transfer in a data communication network," in *Proc. Int. Symp. on Information Theory* (Santa Monica, CA, Feb. 1981).

[87] ———, "Phase noise effects on synchronous network performance," presented at NTC '81, New Orleans, LA, Dec. 1981.

[88] W. C. Lindsey, W. C. Hagmann, and F. Ghazvinian, "Network synchronization techniques: An overview," *NTZ Archiv*, July 1982.

[89] W. C. Lindsey and C. M. Chie, "Theory of oscillator instability based upon structure functions," *Proc. IEEE*, vol. 64, no. 12, pp. 1652–1666, Dec. 1976.

[90] H. J. Choi, "Network synchronization for time transfer applications," Ph.D. dissertation, Dep. Elec. Eng., Univ. of So. Calif., Los Angeles, CA, Sept. 1982.

[91] K. Dessouky, "Nonlinear theory of mutually synchronized oscillators," Ph.D. dissertation, Dep. Elec. Eng., Univ. of So. Calif., Los Angeles, CA, Dec. 1982.

[92] W. R. Braun, "Short term frequency instability effects in networks of coupled oscillators," *IEEE Trans. Commun.*, vol. COM-28, no. 8, pp. 1269–1275, Aug. 1980.

[93] C. E. Ellingson and R. S. Kulpinski, "Dissemination of system time," *IEEE Trans. Commun.*, vol. COM-21, no. 5, pp. 805–824, 1973.

[94] J. W. Schwartz, "Ranging and synchronization between nominally co-orbital satellites," presented at NTC '81, New Orleans, LA, Dec. 1981.

[95] F. Ghazvinian and F. Davarian, "A time synchronization and ranging system," presented at ICC '82, Philadelphia, PA, June 1982.

[96] F. Ghazvinian, "Synchronization in digital communication networks," Ph.D. dissertation, Univ. of So. Calif., Los Angeles, CA, June 1981.

[97] W. C. Hagmann, "Network synchronization techniques for satellite communication systems," Ph.D. dissertation, Univ. of So. Calif., Los Angeles, CA, Aug. 1981.

[98] K. Inagaki *et al.*, "International connection of plesiochronous networks via TDMA satellite link," presented at ICC '82, Philadelphia, PA, June 1982.

[99] P. C. Parks and M. R. Miller, "Stability of PCM characteristic equation," *Electron. Lett.*, no. 12, pp. 468–469, 1966.

[100] M. R. Miller, "Feasibility studies of synchronized systems for PCM telephone networks," *Proc. Inst. Elec. Eng.*, vol. 116, no. 7, pp. 1135–1143, July 1969.

[101] M. R. Miller, P. C. Park, and J. Yamato, "Comments on synchronization of a PCM integrated telephone network," *IEEE Trans. Commun.*, vol. COM-18, no. 3, pp. 269–270, 1970.

[102] D. Mitra, "Network synchronization: Analysis of a hybrid of master-slave and mutual synchronization," *IEEE Trans. Commun.*, vol. COM-28, no. 8, pp. 1245–1259, Aug. 1980.

[103] H. J. Choi and W. C. Lindsey, "Phase and frequency transfer analysis for N mutually synchronized oscillators," *IEEE Trans. Aerosp. Electron. Syst.*, vol. AES-20, no. 6, pp. 748–753, Nov. 1984.